Electronic Supplementary Material

Intercalation-Mediated Activation and Enhancement of Sliding Ferroelectricity in Transition Metal Dichalcogenide Heterobilayers

Dong-Hui Xu[a], Shuangli Yue[a], Li Zhang[a], Gang Jiang[a], Yunpeng Lu[b], Mingli Yang[c] and Xian Wang[a,b]

[a] *Institute of Atomic and Molecular Physics, Key Laboratory of High Energy Density Physics of Ministry of Education, Sichuan University, Chengdu 610065, China*
[b] *School of Chemistry, Chemical Engineering and Biotechnology, Nanyang Technological University, 637371, Singapore*
[c] *Research Center for Materials Genome Engineering, Sichuan University, Chengdu 610065, China*

Contents of the Supporting Information

1. Definition of Insertion Sites in MX_2 Heterobilayers 1
2. Equivariant Distance Computation with PBCs in CEGNN 2
3. Model Training and Evaluation Protocols 3
4. **Table S1.** OOP & Energy Barriers: AB(BA) 6
5. **Table S2.** OOP & Energy Barriers: AC(CA) 7
6. **Table S3.** OOP at Different Intercalation Coverages 8
7. **Table S4.** Convergence Tests of OOP vs. Vacuum Thickness 9
8. **Table S5.** AB(BA) Sliding Ferroelectric OOP 10
9. **Table S6.** AC(CA) Sliding Ferroelectric OOP 14
10. **Table S7.** Bader Charge Variations before and after Intercalation 18
11. **Table S8.** AB(BA) Lattice and Energies 19
12. **Table S9.** AC(CA) Lattice and Energies 28
13. **Table S10.** Five-Number Statistics of Interlayer Distance and Binding Energy 37
14. **Table S11.** Energy Comparison between 2H and 1T Phases 38
15. **Table S12.** AB(BA) Sliding Energy Barriers 39
16. **Table S13.** AC(CA) Sliding Energy Barriers 41
17. **Table S14.** Ten-Fold Cross-Validation Results 43
18. **Figure S1.** OOP Distribution and Sliding Barriers of AB(BA) and AC(CA) Heterobilayers 45
19. **Figure S2.** OOP Distribution of Non-Sliding AB(BA) Heterobilayers 46
20. **Figure S3.** OOP Distribution of Non-Sliding AC(CA) Heterobilayers 47
21. **Figure S4.** Schematic of Intercalation Sites in AB(BA) and AC(CA) Stackings 48
22. **Figure S5.** Comparison of OOP from Different Methods 50
23. **Figure S6.** Translational and Rotational Symmetry under Periodic Boundary Conditions 51
24. **Figure S7.** Non-Switchable OOP in AB(BA) Heterobilayers 52
25. **Figure S8.** Non-Switchable OOP in AC(CA) Heterobilayers 54
26. **Figure S9.** Charge Density Difference before and after Intercalation 56
27. **Figure S10.** Distributions of Interlayer Distance and Binding Energy 57
28. **Figure S11.** Thermal Stability from AIMD Simulations 58

29. **Figure S12.** Phonon Dispersions of Pristine TMD Monolayers.....59
30. **Figure S13.** Structural Schematics before and after Intercalation.....60
31. **Figure S14.** Parity Plot of CEGNN-Predicted and DFT OOP.....61

Method Supplement

1. Definition of Insertion Sites in MX_2 Heterobilayers

To systematically characterize atomic insertion sites in transition metal dichalcogenide (MX_2, M = Ti, Zr, Hf, Cr, Mo; X = S, Se, Te) heterobilayers, we define twelve distinct configurations corresponding to three sites (Site1-Site3) under two stacking orders (e.g., AB vs. BA or AC vs. CA). For each case, the position vector of the inserted atom is given as:

$$r_{atom(Site@Stacking)} = (x, y, z) \quad (S1)$$

Where the in-plane coordinates (x, y) are determined by the top or bottom layer atom (M or X), depending on the specific site definition, specifically:

$$r_{atom(Site1@AB)} = (x_{top\ M}, y_{top\ M}, z) \quad (S2)$$

$$r_{atom(Site1@BA)} = (x_{top\ X}, y_{top\ X}, z) \quad (S3)$$

$$r_{atom(Site2@AB)} = (x_{top\ X}, y_{top\ X}, z) \quad (S4)$$

$$r_{atom(Site2@BA)} = (x_{bottom\ M}, y_{bottom\ M}, z) \quad (S5)$$

$$r_{atom(Site3@AB)} = (x_{bottom\ X}, y_{bottom\ X}, z) \quad (S6)$$

$$r_{atom(Site3@BA)} = (x_{bottom\ X}, y_{bottom\ X}, z) \quad (S7)$$

$$r_{atom(Site1@AC)} = (x_{top\ X}, y_{top\ X}, z) \quad (S8)$$

$$r_{atom(Site1@CA)} = (x_{top\ M}, y_{top\ M}, z) \quad (S9)$$

$$r_{atom(Site2@AC)} = (x_{bottom\ M}, y_{bottom\ X}, z) \quad (S10)$$

$$r_{atom(Site2@CA)} = (x_{bottom\ M}, y_{bottom\ X}, z) \quad (S11)$$

$$r_{atom(Site3@AC)} = (x_{bottom\ X}, y_{bottom\ X}, z) \quad (S12)$$

$$r_{atom(Site3@CA)} = (x_{bottom\ X}, y_{bottom\ X}, z) \quad (S13)$$

and the out-of-plane coordinate z is consistently defined as the average of the minimum and maximum z-coordinates of all X atoms in the Heterobilayers, i.e.,

$$z = \frac{z_{min}^{X} + z_{max}^{X}}{2} \quad (S14)$$

This ensures that the inserted atom is always placed at the vertical center between the two chalcogen layers.

Site1@AB and Site1@BA are mirror-related: inserting an atom at Site1 in AB stacking and performing a lateral sliding yields the Site1 configuration in BA stacking. In these cases, the lateral

position corresponds to the top M atom in AB and the top X atom in BA, respectively.

Site2@AB and Site2@BA are defined such that the inserted atom laterally aligns with the top X atom in AB and the bottom M atom in BA, respectively.

Site3@AB and Site3@BA both position the atom laterally aligned with the bottom X atom, but on opposite stacking sequences.

Similarly, Site1@AC and Site1@CA, Site2@AC and Site2@CA, as well as Site3@AC and Site3@CA, follow the same logic with respect to the AC and CA stacking orders.

2. Incorporating Periodic Boundary Conditions in CEGNN for Equivariant Distance Computation.

In crystalline structures, atomic positions are typically represented using fractional coordinates relative to the lattice vectors. Due to the inherent periodicity of crystals, atoms can interact not only with others within the same unit cell but also with those in adjacent cells through periodic boundaries. To accurately compute interatomic distances in the CEGNN model, it is therefore essential to account for these periodic boundary conditions. The procedure is as follows: first, the fractional coordinates of any two atoms are converted into Cartesian coordinates. Let the fractional coordinates of the two atoms be (u_1,v_1,w_1) and (u_2,v_2,w_2), respectively:

For atom 1

$$\begin{pmatrix} x_1 \\ y_1 \\ z_1 \end{pmatrix} = u_1 a + v_1 b + w_1 c \quad (S15)$$

For atom 2

$$\begin{pmatrix} x_2 \\ y_2 \\ z_2 \end{pmatrix} = u_2 a + v_2 b + w_2 c \quad (S16)$$

The radial distance d_{ij} between two atoms in Cartesian space is

$$d_{ij} = \sqrt{(x_2 - x_1)^2 + (y_2 - y_1)^2 + (z_2 - z_1)^2} \quad (S17)$$

Adjust periodicity for each Cartesian coordinate difference

$$\Delta x = x_2 - x_1 - a \cdot round\left(\frac{x_2 - x_1}{a}\right)$$

$$\Delta y = y_2 - y_1 - b \cdot round(\frac{y_2 - y_1}{b}) \quad (S18)$$

$$\Delta z = z_2 - z_1 - c \cdot round(\frac{z_2 - z_1}{c})$$

Recalculate the radial distance by applying periodicity corrections to each Cartesian coordinate difference

$$d_{ij} = \sqrt{\Delta x^2 + \Delta y^2 + \Delta z^2} \quad (S19)$$

3. Model Training and Evaluation Protocols.

In this study, several evaluation metrics were employed to assess the performance of our model in regression tasks. The following sections provide detailed descriptions of the specific metrics used, along with their corresponding mathematical formulations.

3.1 Data Splitting

The dataset was initially split into training and test sets in a 9:1 ratio, ensuring that the model is trained on a sufficiently large portion of the data while reserving an independent subset for unbiased performance evaluation.

3.2 Training Process

We first trained and evaluated the model using 10-fold cross-validation. For each fold, the model was initialized with two EGNN layers, appropriate data loaders were prepared, and the mean squared error (MSE) was selected as the loss function. The Adam optimizer was used for parameter optimization. The training process was run for a total of 300 epochs. During each epoch, the training loop iterated over the data to perform forward propagation, loss computation, backpropagation, and parameter updates. Simultaneously, model performance on the validation set was evaluated, and the validation loss was recorded. The model parameters yielding the best validation performance were saved. Finally, the best-performing model was reloaded and evaluated on the independent test set.

3.3 Regression Task Evaluation

For the regression task, model performance was evaluated using the coefficient of determination

(R^2), mean absolute error (MAE), and root mean square error (RMSE).

3.3.1 Coefficient of Determination (R^2)

The R^2 score measures the proportion of variance in the target variable that is predictable from the input features. It ranges from negative infinity to 1, where 1 indicates perfect prediction, 0 indicates performance equivalent to predicting the mean, and negative values indicate worse-than-mean performance

$$R^2 = 1 - \frac{\sum_{i=1}^{n}(y_i - \hat{y}_i)^2}{\sum_{i=1}^{n}(y_i - \bar{y}_i)^2} \quad \text{(S20)}$$

Where y_i is the true value, $\hat{y}_i$ is the predicted value, and $\bar{y}_i$ is the mean of the true values.

3.3.2 Mean Absolute Error (MAE)

MAE measures the average magnitude of the absolute differences between predicted and true values. It reflects the average bias in predictions and has the same unit as the target variable

$$MAE = \frac{1}{n}\sum_{i=1}^{n}|y_i - \hat{y}_i| \quad \text{(S21)}$$

Where y_i is the true value, $\hat{y}_i$ is the predicted value.

3.3.3 Root Mean Square Error (RMSE)

RMSE is the square root of the mean of the squared differences between predicted and true values. It penalizes larger errors more heavily and is sensitive to outliers

$$RMSE = \sqrt{\frac{1}{n}\sum_{i=1}^{n}(y_i - \hat{y}_i)^2} \quad \text{(S22)}$$

Where y_i is the true value, $\hat{y}_i$ is the predicted value.

3.4 Target Value Processing

Min-Max Normalization (Min-Max Scaling)

To improve numerical stability and convergence efficiency during model training, all target values were normalized using the Min-Max scaling method. The normalization and inverse transformation are defined as

$$y_{norm} = \frac{y - y_{min}}{y_{max} - y_{min}} \; and \; y = y_{norm} \cdot (y_{max} - y_{min}) + y_{min} \tag{S23}$$

where y is the original target value, y_{norm} is the normalized value, and y_{min}, y_{max} denote the minimum and maximum values of the target variable in the training set. This transformation linearly scales all target values into the range of [0, 1], helping mitigate potential bias caused by large variations in value magnitude. After model prediction, an inverse transformation was applied to recover the physical quantity in its original scale.

Table S1. The sliding out-of-plane polarization (OOP, in pC/m) and energy barriers (E_{bar}, in meV/f.u.) for AB and BA stackings.

Compounds	**AB**	**BA**	E_{bar}
$MoSe_2/WSe_2$	0.12	-0.89	17.60
$HfS_2/TiSe_2$	0.67	-1.76	8.70
$TiTe_2/HfTe_2$	0.37	-1.91	19.40
$MoSe_2/WS_2$	0.95	0.00	18.80
$ZrTe_2/TiTe_2$	1.19	-1.43	8.00
$MoTe_2/CrTe_2$	0.57	-0.20	20.80
HfS_2/ZrS_2	1.19	-0.64	13.70
$ZrS_2/ZrSe_2$	0.20	-1.70	12.30
$HfSe_2/ZrSe_2$	1.55	-0.86	16.20
$WS_2/CrSe_2$	0.01	-0.75	12.70
$HfSe_2/TiSe_2$	1.70	-0.80	10.00
WS_2/MoS_2	0.80	-0.18	15.50
CrS_2/MoS_2	0.17	-1.29	11.50
$ZrS_2/TiSe_2$	0.24	-2.18	7.50
$ZrTe_2/HfTe_2$	1.19	-2.11	15.70
$MoSe_2/CrSe_2$	0.72	-0.07	14.90
$HfS_2/HfSe_2$	0.36	-1.68	13.40

Table S2. The sliding out-of-plane polarization (OOP, in pC/m) and energy barriers (E_{bar}, in meV/f.u.) for AC and CA stackings.

Compounds	**AC**	**CA**	E_{bar}
$MoTe_2/WTe_2$	0.10	-0.95	62.60
$MoTe_2/CrTe_2$	-0.42	0.66	18.60

Table S3. Out-of-plane polarization (OOP, in pC/m) of two representative TMD heterobilayers intercalated by Ag and Ga atom at a coverage of ic-fraction = 1, 0.75, 0.5, 0.25.

	ic-fraction			
	1	**0.75**	**0.5**	**0.25**
AB: HfS_2/ZrS_2(Site1@Ag)	1.527	2.115	1.243	0.57
AB: HfS_2/ZrS_2(Site1@Ga)	1.075	-0.093	0.703	1.679
CA: $MoTe_2/WTe_2$(Site1@Ag)	0.724	-2.441	4.488	3.908
CA: $MoTe_2/WTe_2$(Site1@Ga)	-1.063	-5.732	-3.306	4.118

Table S4. Convergence tests of the out-of-plane polarization (OOP, in pC/m) for six representative TMD heterobilayers with relatively large polarization, evaluated at different vacuum thicknesses (20, 25, and 30 Å). The grey shading highlights the vacuum thickness adopted in this work (~20 Å) and the corresponding OOP value.

	Vacuum thickness (Å)	**OOP (pC/m)**
$MoSe_2/WS_2$	30	0.95
	25	0.95
	20	0.95
$ZrTe_2/TiTe_2$	30	1.19
	25	1.27
	20	1.28
$HfSe_2/ZrSe_2$	30	1.55
	25	1.49
	20	1.48
$HfSe_2/TiSe_2$	30	1.70
	25	1.75
	20	1.64
$ZrS_2/TiSe_2$	30	0.24
	25	0.25
	20	0.23
$ZrTe_2/HfTe_2$	30	1.19
	25	1.15
	20	1.10

Table S5. Among the structures constructed from 47 AB(BA)-stacked heterobilayers via atomic intercalation, 120 exhibit sliding ferroelectric out-of-plane polarization. Positive values denote OOP↑, while negative values denote OOP↓. The sign indicates only the relative polarization direction. OOP values are given in units of pC/m.

	Structure (Site@Intercalated Metal)	AB	BA
1	HfS_2/ZrS_2(Site1@Pt)	6.825	-0.199
2	$ZrS_2/HfSe_2$(Site1@Pt)	0.724	-6.342
3	$HfS_2/HfSe_2$(Site1@Pt)	1.701	-5.470
4	$ZrS_2/ZrSe_2$(Site1@Pt)	1.972	-5.345
5	$TiS_2/TiSe_2$(Site1@Pt)	0.548	-3.859
6	$HfSe_2/TiTe_2$(Site1@Pt)	1.287	-3.592
7	$MoSe_2/CrSe_2$(Site3@Pt)	3.311	-0.021
8	$ZrS_2/TiSe_2$(Site1@Pt)	1.635	-3.304
9	$MoTe_2/CrTe_2$(Site2@Zn)	-0.316	3.263
10	$ZrTe_2/TiTe_2$(Site1@Pt)	3.130	-0.124
11	$ZrTe_2/HfTe_2$(Site1@Pt)	2.969	-2.490
12	$CrSe_2/MoS_2$(Site3@Pt)	2.854	-0.157
13	$HfS_2/TiSe_2$(Site1@Pt)	2.829	-2.179
14	$ZrS_2/HfSe_2$(Site3@Pt)	-2.777	0.058
15	$TiTe_2/HfTe_2$(Site1@Pt)	2.679	-0.679
16	$MoTe_2/WTe_2$(Site1@Pt)	2.632	-1.701
17	$CrSe_2/MoS_2$(Site2@Au)	-0.265	2.631
18	$CrSe_2/MoS_2$(Site1@Au)	2.560	-0.428
19	$MoSe_2/WS_2$(Site3@Pt)	2.497	-0.833
20	$WS_2/CrSe_2$(Site3@Pt)	0.550	-2.459
21	WS_2/MoS_2(Site1@Pt)	-0.440	2.393
22	$ZrS_2/ZrSe_2$(Site3@Pt)	-2.315	1.030
23	WS_2/MoS_2(Site1@Cu)	2.269	-0.441
24	$ZrS_2/TiSe_2$(Site3@Pt)	-2.242	0.710
25	$WS_2/CrSe_2$(Site2@Cu)	-0.338	2.222
26	$MoSe_2/WS_2$(Site2@Cu)	-2.198	1.252
27	WS_2/MoS_2(Site3@Pt)	2.182	-1.634
28	$MoTe_2/WTe_2$(Site3@Au)	2.149	-1.830
29	$HfSe_2/TiTe_2$(Site3@Pt)	-2.124	0.755
30	$MoSe_2/MoS_2$(Site2@Au)	-0.032	2.115

31	$HfS_2/HfSe_2$(Site3@Pt)	-2.103	0.834
32	$CrSe_2/MoS_2$(Site2@Cu)	-1.286	2.012
33	$CrSe_2/MoS_2$(Site2@Zn)	-1.999	0.426
34	$MoSe_2/WS_2$(Site1@Pt)	-1.993	1.110
35	$MoTe_2/WTe_2$(Site3@Cu)	1.243	-1.976
36	$CrSe_2/MoS_2$(Site2@Ag)	-0.212	1.944
37	$MoTe_2/WTe_2$(Site3@Ag)	0.796	-1.941
38	$MoTe_2/CrTe_2$(Site2@Ag)	-0.012	1.937
39	$ZrTe_2/HfTe_2$(Site3@Au)	-0.149	1.877
40	$HfS_2/TiSe_2$(Site3@Pt)	-1.454	1.875
41	$MoSe_2/WS_2$(Site2@Au)	-1.858	0.579
42	$MoSe_2/CrSe_2$(Site1@Pt)	-1.213	1.841
43	$ZrTe_2/TiTe_2$(Site3@Pt)	-0.341	1.831
44	$MoTe_2/CrTe_2$(Site1@Zn)	1.770	-0.731
45	$WS_2/CrSe_2$(Site1@Cu)	0.789	-1.748
46	$MoTe_2/CrTe_2$(Site2@Au)	-1.746	1.082
47	$ZrTe_2/HfTe_2$(Site1@Au)	0.055	-1.721
48	$MoTe_2/WTe_2$(Site3@Pt)	0.208	-1.697
49	$MoSe_2/CrSe_2$(Site2@Au)	-1.666	0.084
50	$MoSe_2/WS_2$(Site1@Au)	0.599	-1.661
51	$CrSe_2/MoS_2$(Site1@Pt)	-0.445	1.632
52	$ZrTe_2/TiTe_2$(Site2@Hg)	-0.011	1.619
53	$CrSe_2/MoS_2$(Site1@Ag)	1.614	-0.237
54	$ZrTe_2/HfTe_2$(Site2@Hg)	-0.244	1.600
55	$CrSe_2/MoS_2$(Site2@Hg)	-1.593	0.527
56	$MoSe_2/WS_2$(Site2@Zn)	-1.579	0.728
57	$WS_2/CrSe_2$(Site2@Ag)	-1.559	0.311
58	$WS_2/CrSe_2$(Site1@Ag)	0.037	-1.540
59	$CrSe_2/MoS_2$(Site1@Cu)	0.635	-1.534
60	WS_2/MoS_2(Site1@Zn)	1.531	-0.274
61	$MoTe_2/WTe_2$(Site3@Cd)	1.274	-1.510
62	$TiTe_2/HfTe_2$(Site3@Pt)	-1.491	1.150
63	$HfS_2/TiSe_2$(Site3@Cu)	-1.490	0.603
64	WS_2/MoS_2(Site2@Au)	-0.752	1.485
65	$ZrTe_2/HfTe_2$(Site3@Cu)	-0.584	1.477
66	$MoSe_2/WS_2$(Site1@Ag)	0.261	-1.468

67	$MoTe_2/WTe_2$(Site3@Hg)	1.465	-0.456
68	$HfSe_2/TiSe_2$(Site2@Cd)	-0.023	1.465
69	$ZrTe_2/TiTe_2$(Site2@Zn)	-1.464	0.454
70	$MoSe_2/WS_2$(Site2@Hg)	-1.414	0.677
71	$MoTe_2/CrTe_2$(Site1@Ag)	1.410	-0.244
72	$MoTe_2/CrTe_2$(Site1@Au)	1.369	-1.069
73	$MoTe_2/CrTe_2$(Site2@Hg)	-1.340	0.466
74	$HfS_2/TiSe_2$(Site3@Au)	-1.313	0.923
75	$ZrTe_2/HfTe_2$(Site1@Cu)	0.160	-1.308
76	$MoSe_2/WS_2$(Site2@Ag)	-1.305	0.550
77	$MoTe_2/WTe_2$(Site3@Zn)	1.261	-0.800
78	$ZrTe_2/TiTe_2$(Site1@Au)	1.251	-0.275
79	$MoSe_2/CrSe_2$(Site1@Au)	0.150	-1.236
80	WS_2/MoS_2(Site1@Au)	1.228	-0.907
81	$ZrTe_2/HfTe_2$(Site3@Zn)	-0.836	1.226
82	HfS_2/ZrS_2(Site2@Ag)	-1.213	0.180
83	$MoTe_2/CrTe_2$(Site1@Cu)	1.201	-0.037
84	$ZrTe_2/TiTe_2$(Site2@Cd)	-1.196	0.354
85	$MoSe_2/MoS_2$(Site1@Hg)	1.160	-0.104
86	$MoTe_2/CrTe_2$(Site1@Hg)	0.256	-1.150
87	$TiTe_2/HfTe_2$(Site3@Au)	-0.396	1.138
88	$CrTe_2/WTe_2$(Site3@Hg)	0.297	-1.122
89	$TiTe_2/HfTe_2$(Site3@Cu)	-1.103	0.703
90	$HfSe_2/TiSe_2$(Site2@Au)	-1.085	0.953
91	HfS_2/ZrS_2(Site1@Ga)	1.075	-0.130
92	$ZrTe_2/TiTe_2$(Site3@Cd)	-0.236	1.064
93	$WS_2/CrSe_2$(Site1@Hg)	0.934	-0.255
94	WS_2/WSe_2(Site2@Pt)	-0.906	0.586
95	$ZrTe_2/HfTe_2$(Site3@Hg)	0.497	-0.880
96	$ZrTe_2/HfTe_2$(Site2@Ga)	0.120	-0.863
97	$HfSe_2/ZrSe_2$(Site2@Ag)	-0.847	0.587
98	$TiTe_2/HfTe_2$(Site3@Zn)	-0.840	0.352
99	$ZrTe_2/HfTe_2$(Site3@Ag)	-0.369	0.816
100	$CrSe_2/MoS_2$(Site2@Ga)	-0.016	0.811
101	WS_2/MoS_2(Site1@Hg)	0.799	-0.676
102	$MoSe_2/WS_2$(Site2@Ga)	-0.745	0.141

103	$MoSe_2/WS_2$(Site2@Cd)	-0.382	0.734
104	$CrSe_2/MoS_2$(Site2@In)	-0.159	0.687
105	HfS_2/ZrS_2(Site1@Hg)	-0.679	0.010
106	$TiTe_2/HfTe_2$(Site3@Cd)	-0.385	0.599
107	$ZrTe_2/TiTe_2$(Site3@Hg)	0.436	-0.596
108	$HfSe_2/TiSe_2$(Site2@Cu)	-0.347	0.561
109	$MoSe_2/WS_2$(Site1@Cd)	0.107	-0.512
110	$MoTe_2/CrTe_2$(Site1@Pt)	0.036	-0.497
111	$ZrTe_2/TiTe_2$(Site1@Ga)	-0.319	0.467
112	$ZrTe_2/TiTe_2$(Site3@In)	0.453	-0.246
113	$TiTe_2/HfTe_2$(Site2@Hg)	-0.427	0.090
114	$TiTe_2/ZrSe_2$(Site2@Pt)	0.404	-0.171
115	$CrSe_2/MoS_2$(Site1@In)	0.232	-0.393
116	$CrSe_2/MoS_2$(Site1@Ga)	0.356	-0.044
117	HfS_2/ZrS_2(Site2@In)	0.355	-0.104
118	CrS_2/MoS_2(Site2@Pt)	0.263	-0.352
119	$CrSe_2/WSe_2$(Site3@Au)	-0.003	0.347
120	$ZrTe_2/TiTe_2$(Site2@In)	0.276	-0.032

Table S6. Among the structures constructed from 47 AC(CA)-stacked heterobilayers via atomic intercalation, 114 exhibit sliding ferroelectric out-of-plane polarization. Positive values denote OOP↑, while negative values denote OOP↓. The sign indicates only the relative polarization direction. OOP values are given in units of pC/m.

	Structure (Site@Intercalated Metal)	AC	CA
1	$CrTe_2/WTe_2$(Site1@Au)	-6.827	0.449
2	$MoTe_2/WTe_2$(Site1@Au)	-5.774	2.561
3	$ZrS_2/HfSe_2$(Site1@Pt)	-5.638	0.736
4	WS_2/WSe_2(Site2@Pt)	-5.205	0.832
5	$HfS_2/HfSe_2$(Site1@Pt)	-4.759	1.374
6	$MoTe_2/WTe_2$(Site1@Cu)	-4.710	0.671
7	$MoTe_2/WTe_2$(Site1@Ag)	-4.547	0.724
8	$ZrS_2/ZrSe_2$(Site1@Pt)	-4.450	1.054
9	WS_2/MoS_2(Site2@Pt)	-0.602	4.352
10	$CrSe_2/WSe_2$(Site3@Au)	0.059	-4.291
11	HfS_2/ZrS_2(Site2@Pt)	0.994	-4.061
12	$TiS_2/TiSe_2$(Site1@Pt)	-3.667	0.023
13	$MoTe_2/WTe_2$(Site1@Cd)	-3.542	1.205
14	$HfSe_2/TiSe_2$(Site2@Pt)	1.564	-3.542
15	HfS_2/ZrS_2(Site1@Au)	-0.470	3.476
16	CrS_2/MoS_2(Site3@Au)	0.659	-3.457
17	$ZrTe_2/TiTe_2$(Site2@Pt)	0.299	-3.419
18	$HfSe_2/ZrSe_2$(Site2@Pt)	1.115	-3.229
19	$TiTe_2/HfTe_2$(Site1@Pt)	-0.509	2.972
20	$HfSe_2/ZrSe_2$(Site1@Au)	-0.312	2.822
21	WS_2/WSe_2(Site3@Cu)	0.020	-2.781
22	WS_2/WSe_2(Site3@Au)	0.421	-2.768
23	WS_2/MoS_2(Site1@Pt)	2.747	-0.692
24	$ZrS_2/TiSe_2$(Site1@Pt)	-2.718	1.095
25	$MoTe_2/WTe_2$(Site1@Zn)	-2.555	1.115
26	$CrSe_2/MoS_2$(Site1@Au)	-0.475	2.502
27	$MoSe_2/CrSe_2$(Site2@Pt)	-1.659	2.430
28	WS_2/MoS_2(Site1@Hg)	-0.678	2.389
29	HfS_2/ZrS_2(Site2@Au)	0.844	-2.365
30	$CrTe_2/WTe_2$(Site1@Hg)	-2.321	0.924

31	WS_2/MoS_2(Site1@Cu)	-0.490	2.319
32	$MoSe_2/WS_2$(Site1@Pt)	2.002	-2.294
33	$TiTe_2/HfTe_2$(Site1@Au)	-2.268	0.880
34	$MoTe_2/WTe_2$(Site3@Pt)	0.490	-2.263
35	$MoTe_2/WTe_2$(Site1@Hg)	-2.250	1.488
36	$WS_2/CrSe_2$(Site2@Pt)	-2.246	1.316
37	$HfSe_2/TiSe_2$(Site2@Cu)	2.198	-0.039
38	$MoSe_2/WSe_2$(Site3@Cu)	0.716	-2.151
39	WS_2/WSe_2(Site3@Zn)	0.627	-2.146
40	HfS_2/ZrS_2(Site1@Cd)	-0.162	2.104
41	$WS_2/CrSe_2$(Site1@Cu)	-2.099	0.886
42	$ZrTe_2/HfTe_2$(Site1@Au)	-2.059	0.905
43	$HfSe_2/TiSe_2$(Site2@Au)	2.041	-0.389
44	$CrSe_2/MoS_2$(Site1@Pt)	1.963	-1.012
45	$ZrTe_2/HfTe_2$(Site1@Pt)	-1.912	1.672
46	$MoSe_2/WSe_2$(Site3@Au)	1.669	-1.910
47	$CrSe_2/MoS_2$(Site3@Zn)	1.908	-0.887
48	$MoSe_2/CrSe_2$(Site1@Pt)	1.890	-1.630
49	$TiTe_2/HfTe_2$(Site3@Au)	0.011	-1.790
50	$CrSe_2/MoS_2$(Site3@Hg)	1.773	-0.446
51	$MoSe_2/WSe_2$(Site3@Ag)	0.464	-1.767
52	$TiTe_2/HfTe_2$(Site1@Cu)	-1.719	0.429
53	$ZrTe_2/TiTe_2$(Site2@Au)	0.896	-1.707
54	$MoSe_2/WS_2$(Site1@Au)	-1.705	0.621
55	$MoTe_2/CrTe_2$(Site1@Zn)	-0.120	1.702
56	$HfS_2/TiSe_2$(Site1@Pt)	-1.482	1.699
57	$ZrTe_2/TiTe_2$(Site1@Au)	-0.551	1.688
58	$CrSe_2/MoS_2$(Site1@Cu)	-1.670	0.651
59	$CrSe_2/MoS_2$(Site1@Ag)	-0.244	1.652
60	HfS_2/ZrS_2(Site2@Zn)	1.002	-1.637
61	$WS_2/CrSe_2$(Site1@Ag)	-1.584	0.024
62	$ZrTe_2/HfTe_2$(Site1@Ag)	-1.551	0.040
63	$MoSe_2/WS_2$(Site1@Ag)	-1.484	0.310
64	$HfSe_2/ZrSe_2$(Site1@Cd)	-0.048	1.478
65	$MoSe_2/WSe_2$(Site3@Zn)	1.282	-1.457
66	$MoTe_2/CrTe_2$(Site1@Au)	-1.414	1.268

67	WS_2/MoS_2(Site1@Zn)	-0.297	1.405
68	WS_2/WSe_2(Site3@Hg)	0.835	-1.354
69	MoSe2/WSe_2(Site3@Hg)	1.347	-0.744
70	$MoTe_2/CrTe_2$(Site1@Ag)	-0.269	1.337
71	$MoSe_2/CrSe_2$(Site1@Au)	-1.313	0.156
72	$MoTe_2/CrTe_2$(Site1@Hg)	-1.311	0.177
73	$MoSe_2/MoS_2$(Site1@Hg)	-0.074	1.272
74	WS_2/MoS_2(Site1@Au)	-0.939	1.237
75	$ZrTe_2/TiTe_2$(Site2@Cu)	0.903	-1.224
76	$HfSe_2/ZrSe_2$(Site2@Zn)	1.220	-0.682
77	$ZrTe_2/HfTe_2$(Site1@Cu)	-1.178	0.717
78	$MoTe_2/CrTe_2$(Site1@Cu)	-0.035	1.173
79	$HfSe_2/ZrSe_2$(Site2@Cd)	1.151	-0.042
80	$ZrTe_2/TiTe_2$(Site2@Hg)	-0.106	1.108
81	$ZrTe_2/HfTe_2$(Site2@Hg)	-0.431	1.058
82	HfS_2/ZrS_2(Site2@Cd)	1.050	-0.886
83	$ZrTe_2/HfTe_2$(Site3@Au)	0.328	-1.041
84	$ZrTe_2/TiTe_2$(Site2@Ag)	1.034	-0.389
85	$MoTe_2/CrTe_2$(Site1@Pt)	0.133	-1.021
86	HfS_2/ZrS_2(Site2@Cu)	0.795	-0.955
87	$HfSe_2/ZrSe_2$(Site2@Au)	0.809	-0.955
88	$CrSe_2/MoS_2$(Site3@In)	0.889	-0.099
89	$HfSe_2/ZrSe_2$(Site2@Cu)	0.836	-0.661
90	$WS_2/CrSe_2$(Site1@Hg)	-0.395	0.833
91	$ZrTe_2/TiTe_2$(Site3@Zn)	0.799	-0.355
92	HfS_2/ZrS_2(Site2@Ag)	0.776	-0.187
93	$ZrTe_2/TiTe_2$(Site3@Hg)	0.772	-0.457
94	$ZrTe_2/HfTe_2$(Site3@Hg)	0.768	-0.652
95	$CrSe_2/MoS_2$(Site2@Zn)	-0.199	0.634
96	$MoSe_2/WS_2$(Site3@Ga)	0.629	-0.133
97	$MoSe_2/WS_2$(Site3@In)	0.628	-0.264
98	$ZrTe_2/TiTe_2$(Site2@Zn)	0.624	-0.094
99	$CrSe_2/MoS_2$(Site3@Ga)	-0.360	0.584
100	$CrTe_2/WTe_2$(Site3@Au)	-0.576	0.464
101	$CrSe_2/MoS_2$(Site2@Hg)	-0.101	0.543
102	$ZrTe_2/TiTe_2$(Site1@Ga)	0.512	-0.207

103	$ZrTe_2/TiTe_2$(Site3@Pt)	-0.498	0.432
104	$MoSe_2/WS_2$(Site1@Cd)	-0.493	0.178
105	$ZrTe_2/TiTe_2$(Site1@Zn)	-0.422	0.164
106	$ZrTe_2/TiTe_2$(Site3@Cd)	0.071	-0.413
107	$CrSe_2/MoS_2$(Site1@In)	-0.349	0.231
108	$CrSe_2/MoS_2$(Site1@Ga)	-0.022	0.269
109	$WS_2/CrSe_2$(Site2@Ag)	-0.125	0.267
110	$ZrTe_2/TiTe_2$(Site3@In)	0.247	-0.028
111	$MoSe_2/CrSe_2$(Site2@Au)	-0.181	0.062
112	$MoSe_2/WS_2$(Site2@In)	0.104	-0.048
113	$MoSe_2/WS_2$(Site2@Ga)	-0.080	0.092
114	CrS_2/MoS_2(Site2@Au)	0.027	-0.019

Table S7. Bader charge variations for the top TMD layer (Q_T), the intercalated metal atom (Q_A), and the bottom TMD layer (Q_B) in representative heterobilayers, for both pristine and metal-intercalated configurations. The values represent net charge deviations with respect to neutral atoms (in units of e). "/" denotes the absence of an intercalated atom in the pristine structures. Each pair of rows corresponds to the same heterobilayer before and after metal intercalation. The positive value represents the extent of electron accumulation. The negative value represents the extent of electron depletion.

	$Q_T(e)$	$Q_A(e)$	$Q_B(e)$
HfS_2/ZrS_2	0.0047	/	-0.0047
HfS_2/ZrS_2(Site1@Pt)	0.0439	-0.2122	0.1683
$ZrS_2/HfSe_2$	-0.0128	/	0.0128
$ZrS_2/HfSe_2$(Site1@Pt)	0.0278	0.1010	-0.1288
WS_2/MoS_2	0.0008	/	-0.0008
WS_2/MoS_2(Site2@Pt)	0.0254	-0.0287	0.0033
$CrTe_2/WTe_2$	-0.0023	/	0.0023
$CrTe_2/WTe_2$(Site1@Au)	-0.1632	0.2197	-0.0565

Table S8. AB(BA) lattice and binding energy and formation energy.

Heterostructures	Type	lattice parameter: a=b (Å)	lattice parameter: gamma (°)	Interlayer distance (Å)	Binding energy ($meV/Å^2$)	Formation energy (meV)
$TiS_2/TiSe_2$(Site1@Pt)	AB	3.47	120.00	3.21	-350.36	-690.03
	BA	3.57	120.00	3.49	-373.58	-723.57
$HfS_2/TiSe_2$(Site1@Pt)	AB	3.53	120.00	3.21	-322.27	-463.56
	BA	3.67	120.00	3.31	-361.35	-604.50
$HfS_2/TiSe_2$(Site3@Cu)	AB	3.53	120.00	3.59	-270.82	1546.39
	BA	3.53	120.00	3.52	-291.68	1470.69
$HfS_2/TiSe_2$(Site3@Au)	AB	3.52	120.00	4.27	-189.64	-678.07
	BA	3.53	120.00	4.16	-201.82	-806.57
$HfS_2/TiSe_2$(Site3@Pt)	AB	3.51	120.00	3.93	-313.31	-505.60
	BA	3.53	120.00	3.78	-373.66	-1125.39
$MoTe_2/WTe_2$(Site1@Pt)	AB	3.51	120.00	4.54	-254.49	97.39
	BA	3.47	120.00	5.02	-320.88	-614.66
$MoTe_2/WTe_2$(Site3@Cu)	AB	3.49	120.00	4.34	-155.7	2102.40
	BA	3.50	120.00	4.93	-150.43	2119.27
$MoTe_2/WTe_2$(Site3@Ag)	AB	3.50	120.00	5.09	-97.33	1748.44
	BA	3.50	120.00	5.41	-101.3	1700.98
$MoTe_2/WTe_2$(Site3@Zn)	AB	3.50	120.00	6.57	-71.84	-243.53
	BA	3.50	120.00	6.89	-61.55	-131.82
$MoTe_2/WTe_2$(Site3@Au	AB	3.49	120.00	4.98	-136.71	-186.76
	BA	3.50	120.00	5.29		

)

$MoTe_2/WTe_2$(Site3@Cd)	AB	3.50	120.00	6.46	-65.95	-458.57
	BA	3.49	120.00	6.60	-59.54	-382.51
$MoTe_2/WTe_2$(Site3@Hg	AB	3.51	120.00	6.75	-58.88	-620.97
	BA	3.51	120.00	7.16		
					-50.14	-526.94
)						
$MoTe_2/WTe_2$(Site3@Pt)	AB	3.47	120.00	4.48	-316.47	-557.45
	BA	3.47	120.00	5.02	-320.89	-614.65
$TiTe_2/HfTe_2$(Site1@Pt)	AB	3.85	120.00	3.28	-370.11	-1045.22
	BA	3.97	120.00	3.77	-366.43	-873.30
$TiTe_2/HfTe_2$(Site2@Hg)	AB	3.79	120.00	6.69	-45.08	-504.40
	BA	3.79	120.00	6.11	-55.44	-631.50
$TiTe_2/HfTe_2$(Site3@Cu)	AB	3.83	120.00	3.89	-234.16	1325.80
	BA	3.84	120.00	3.77	-254.52	1035.40
$TiTe_2/HfTe_2$(Site3@Zn)	AB	3.84	120.00	4.23	-99.09	-943.51
	BA	3.88	120.00	4.06	-104.23	-1039.72
$TiTe_2/HfTe_2$(Site3@Au)	AB	3.82	120.00	4.49	-202.87	-685.54
	BA	3.85	120.00	4.35	-213.97	-835.37
$TiTe_2/HfTe_2$(Site3@Cd)	AB	3.86	120.00	4.89	-68.39	-700.27
	BA	3.90	120.00	4.74	-71.65	-712.68
$TiTe_2/HfTe_2$(Site3@Pt)	AB	4.00	120.00	3.68	-358.22	-681.39
	BA	3.84	120.00	3.96	-383.84	-1250.69
$MoSe_2/WS_2$(Site1@Ag)	AB	3.20	120.00	5.44	-81.18	2071.61
	BA	3.20	120.00	5.17	-90.43	2016.34
$MoSe_2/WS_2$(Site1@Au)	AB	3.17	120.00	5.70	-93.56	-49.98
	BA	3.19	120.00	5.30	-105.79	-158.98
$MoSe_2/WS_2$(Site1@Cd)	AB	3.21	120.00	6.16	-77.58	-464.94

	BA	3.21	120.00	6.08	-78.67	-474.11
$MoSe_2/WS_2$(Site1@Pt)	AB	3.21	120.00	4.26	-177.81	393.72
	BA	3.17	120.00	4.40	-259.26	-374.26
$MoSe_2/WS_2$(Site2@Cu)	AB	3.22	120.00	4.00	-151.12	2217.33
	BA	3.21	120.00	3.75	-121.81	2578.06
$MoSe_2/WS_2$(Site2@Ag)	AB	3.20	120.00	5.36	-87.9	2056.07
	BA	3.20	120.00	5.44	-80.62	2088.11
$MoSe_2/WS_2$(Site2@Ga)	AB	3.21	120.00	5.89	-77.76	-330.13
	BA	3.21	120.00	5.75	-75.73	-310.29
$MoSe_2/WS_2$(Site2@Zn)	AB	3.21	120.00	5.76	-68.96	-490.08
	BA	3.21	120.00	5.68	-72.5	-524.04
$MoSe_2/WS_2$(Site2@Au)	AB	3.18	120.00	5.40	-102.59	-130.73
	BA	3.17	120.00	5.73	-93.35	-48.10
$MoSe_2/WS_2$(Site2@Cd)	AB	3.21	120.00	6.14	-76.7	-456.87
	BA	3.22	120.00	6.13	-77.02	-460.43
$MoSe_2/WS_2$(Site2@Hg)	AB	3.23	120.00	6.40	-68.88	-476.29
	BA	3.23	120.00	6.16	-75.58	-537.76
$MoSe_2/WS_2$(Site3@Pt)	AB	3.17	120.00	4.42	-235.49	-164.47
	BA	3.21	120.00	4.23	-227.4	-54.10
$ZrTe_2/TiTe_2$(Site1@Ga)	AB	3.88	120.00	4.07	-159.55	-1009.16
	BA	3.84	120.00	5.34	-119.85	-545.49
$ZrTe_2/TiTe_2$(Site1@Au)	AB	3.86	120.00	3.81	-183.65	-444.10
	BA	3.85	120.00	4.44	-207.08	-712.88
$ZrTe_2/TiTe_2$(Site1@Pt)	AB	3.87	120.00	3.26	-373.35	-1059.12
	BA	4.04	120.00	3.60	-376	-900.33
$ZrTe_2/TiTe_2$(Site2@In)	AB	3.82	120.00	5.80	-107.63	-890.77
	BA	3.86	120.00	4.98	-123.42	-1078.06
$ZrTe_2/TiTe_2$(Site2@Zn)	AB	3.91	120.00	4.00	-115.09	-1168.87
	BA	3.86	120.00	3.67	-103.03	-1066.56

$ZrTe_2/TiTe_2$(Site2@Cd)	AB	3.93	120.00	4.65	-81.29	-800.89
	BA	3.90	120.00	4.24	-80.75	-875.85
$ZrTe_2/TiTe_2$(Site2@Hg)	AB	3.81	120.00	6.68	-44.82	-480.50
	BA	3.81	120.00	6.09	-54.32	-601.67
$ZrTe_2/TiTe_2$(Site3@In)	AB	3.82	120.00	6.20	-105.91	-871.15
	BA	3.83	120.00	5.77	-108.66	-901.50
$ZrTe_2/TiTe_2$(Site3@Cd)	AB	3.89	120.00	4.84	-69.8	-725.66
	BA	3.93	120.00	4.71	-74.28	-741.67
$ZrTe_2/TiTe_2$(Site3@Hg)	AB	3.81	120.00	6.40	-47.25	-509.63
	BA	3.81	120.00	6.60	-45.08	-484.60
$ZrTe_2/TiTe_2$(Site3@Pt)	AB	4.00	120.00	3.73	-371.42	-927.21
	BA	3.88	120.00	3.93	-390.05	-1318.59
$MoTe_2/CrTe_2$(Site1@Cu)	AB	3.52	120.00	3.74	-177.89	1950.71
	BA	3.51	120.00	4.26	-182.72	1899.54
$MoTe_2/CrTe_2$(Site1@Ag)	AB	3.51	120.00	4.69	-102.34	1639.68
	BA	3.51	120.00	5.03	-113.05	1631.17
$MoTe_2/CrTe_2$(Site1@Zn)	AB	3.53	120.00	4.74	-55.88	-56.70
	BA	3.50	120.00	6.57	-74.31	-265.51
$MoTe_2/CrTe_2$(Site1@Au)	AB	3.50	120.00	4.60	-128.09	-81.52
	BA	3.51	120.00	4.90	-152.6	-316.28
$MoTe_2/CrTe_2$(Site1@Hg	AB	3.50	120.00	6.44	-68.25	-712.47
	BA		120.00			

)

$MoTe_2/CrTe_2$(Site1@Pt)	AB	3.52	120.00	3.92	-304.97	-384.48
	BA	3.49	120.00	4.43	-328.55	-674.95
$MoTe_2/CrTe_2$(Site2@Ag	AB	3.51	120.00	5.07	-105.4	1713.05
	BA		120.00			
		3.50		4.76	-99.81	1693.66
)						
$MoTe_2/CrTe_2$(Site2@Zn)	AB	3.49	120.00	6.57	-75.2	-274.77
	BA	3.52	120.00	4.74	-56.68	-60.96
$MoTe_2/CrTe_2$(Site2@Au	AB	3.51	120.00	5.01	-136.7	-156.44
	BA		120.00			
		3.50		4.68	-125.36	-60.07
)						
$MoTe_2/CrTe_2$(Site2@Hg	AB	3.50	120.00	6.71	-60.92	-631.22
	BA		120.00			
		3.50		6.45	-68.56	-713.32
)						
HfS_2/ZrS_2(Site1@Ga)	AB	3.54	120.00	4.16	-162.67	-1040.12
	BA	3.53	120.00	5.54	-141.69	-882.41
HfS_2/ZrS_2(Site1@Hg)	AB	3.53	120.00	5.87	-56.78	-598.26
	BA	3.53	120.00	6.09	-52.57	-549.10
HfS_2/ZrS_2(Site1@Pt)	AB	3.54	120.00	3.03	-331.76	-572.58
	BA	3.68	120.00	3.18	-358.09	-660.00
HfS_2/ZrS_2(Site2@Ag)	AB	3.55	120.00	4.07	-193.32	969.09
	BA	3.55	120.00	3.62	-182.63	1062.63
HfS_2/ZrS_2(Site2@In)	AB	3.52	120.00	5.55	-131.87	-1218.66
	BA	3.54	120.00	4.82	-137.43	-1251.31
$ZrS_2/ZrSe_2$(Site1@Pt)	AB	3.65	120.00	2.98	-341.34	-563.48

	BA	3.76	120.00	3.20	-379.38	-928.08
$ZrS_2/ZrSe_2$(Site3@Pt)	AB	3.76	120.00	3.39	-340.81	-456.00
	BA	3.64	120.00	3.70	-372.23	-1055.82
WS_2/WSe_2(Site2@Pt)	AB	3.21	120.00	4.24	-223.02	-19.27
	BA	3.21	120.00	4.28	-177.53	390.06
$HfSe_2/ZrSe_2$(Site2@Ag)	AB	3.69	120.00	4.24	-170.97	987.12
	BA	3.69	120.00	3.73	-165.34	1034.9
$WS_2/CrSe_2$(Site1@Cu)	AB	3.18	120.00	3.75	-128.5	2483.77
	BA	3.15	120.00	4.17	-142.98	2538.82
$WS_2/CrSe_2$(Site1@Ag)	AB	3.15	120.00	5.56	-81.83	1967.99
	BA	3.15	120.00	5.31	-90.06	1941.62
$WS_2/CrSe_2$(Site1@Hg)	AB	3.19	120.00	6.19	-77.57	-568.15
	BA	3.18	120.00	6.31	-72.71	-523.75
$WS_2/CrSe_2$(Site2@Cu)	AB	3.17	120.00	3.99	-142.14	2547.12
	BA	3.17	120.00	3.67	-126.66	2522.04
$WS_2/CrSe_2$(Site2@Ag)	AB	3.15	120.00	5.47	-88.12	1957.66
	BA	3.15	120.00	5.52	-81.83	1978.91
$WS_2/CrSe_2$(Site3@Pt)	AB	3.13	120.00	4.42	-264.63	-606.59
	BA	3.14	120.00	4.45	-249.46	-468.01
$HfSe_2/TiSe_2$(Site2@Cu)	AB	3.59	120.00	3.59	-277	1225.14
	BA	3.58	120.00	3.13	-250.39	1817.76
$HfSe_2/TiSe_2$(Site2@Au)	AB	3.60	120.00	4.25	-198.74	-656.62
	BA	3.61	120.00	3.78	-152.34	-138.42
$HfSe_2/TiSe_2$(Site2@Cd)	AB	3.65	120.00	4.47	-87.96	-715.89
	BA	3.65	120.00	3.93	-94.41	-800.78
$ZrS_2/HfSe_2$(Site1@Pt)	AB	3.63	120.00	3.02	-329.11	-464.08
	BA	3.74	120.00	3.23	-371.11	-850.81
$ZrS_2/HfSe_2$(Site3@Pt)	AB	3.61	120.00	3.89	-302.69	-300.20
	BA	3.62	120.00	3.72	-360	-944.13

$HfSe_2/TiTe_2$(Site1@Pt)	AB	3.73	120.00	3.36	-340.88	-636.48
	BA	3.88	120.00	3.45	-351.87	-503.14
$HfSe_2/TiTe_2$(Site3@Pt)	AB	3.71	120.00	4.02	-331.55	-603.47
	BA	3.73	120.00	3.91	-383.78	-1212.21
$CrSe_2/WSe_2$(Site3@Au)	AB	3.21	120.00	5.32	-111.36	-208.59
	BA	3.21	120.00	5.47	-106.84	-168.42
WS_2/MoS_2(Site1@Cu)	AB	3.15	120.00	3.61	-133.92	2515.13
	BA	3.14	120.00	4.07	-147.48	2585.30
WS_2/MoS_2(Site1@Zn)	AB	3.15	120.00	5.61	-75.46	-106.38
	BA	3.14	120.00	5.64	-75.47	-99.82
WS_2/MoS_2(Site1@Au)	AB	3.12	120.00	5.69	-90.28	-173.84
	BA	3.13	120.00	5.31	-101.23	-268.28
WS_2/MoS_2(Site1@Hg)	AB	3.18	120.00	6.09	-76.38	-548.69
	BA	3.17	120.00	6.25	-70.94	-499.94
WS_2/MoS_2(Site1@Pt)	AB	3.14	120.00	4.37	-167.23	237.18
	BA	3.12	120.00	4.36	-245.28	-466.93
WS_2/MoS_2(Site2@Au)	AB	3.13	120.00	5.40	-98.77	-247.26
	BA	3.12	120.00	5.69	-89.9	-170.80
WS_2/MoS_2(Site3@Pt)	AB	3.12	120.00	4.35	-242.87	-428.96
	BA	3.13	120.00	4.32	-228.92	-304.79
$CrTe_2/WTe_2$(Site3@Hg)	AB	3.50	120.00	6.72	-60.59	-627.55
	BA	3.50	120.00	7.13	-51.78	-533.69
CrS_2/MoS_2(Site2@Pt)	AB	3.07	120.00	4.32	-242.42	-482.82
	BA	3.08	120.00	4.41	-183.46	19.91
$TiTe_2/ZrSe_2$(Site2@Pt)	AB	3.76	120.00	3.88	-386.97	-1272.91
	BA	3.75	120.00	3.25	-354.3	-787.59
$ZrS_2/TiSe_2$(Site1@Pt)	AB	3.56	120.00	3.11	-341.31	-623.59
	BA	3.69	120.00	3.29	-381.84	-869.70
$ZrS_2/TiSe_2$(Site3@Pt)	AB	3.54	120.00	3.86	-320.02	-537.10

	BA	3.56	120.00	3.76	-379.15	-1162.08
$MoSe_2/MoS_2$(Site1@Hg)	AB	3.23	120.00	6.12	-76.02	-538.01
	BA	3.23	120.00	6.33	-70.42	-486.12
$MoSe_2/MoS_2$(Site2@Au)	AB	3.19	120.00	5.39	-102.85	-132.04
	BA	3.17	120.00	5.72	-91.03	-26.97
$ZrTe_2/HfTe_2$(Site1@Cu)	AB	3.89	120.00	3.24	-223.22	2887.77
	BA	3.92	120.00	3.75	-234.28	2755.15
$ZrTe_2/HfTe_2$(Site1@Au)	AB	3.92	120.00	3.75	-176.27	-411.30
	BA	3.91	120.00	4.37	-195.16	-638.51
$ZrTe_2/HfTe_2$(Site1@Pt)	AB	3.91	120.00	3.20	-361.02	-1015.23
	BA	4.09	120.00	3.52	-367.86	-943.02
$ZrTe_2/HfTe_2$(Site2@Ga)	AB	3.89	120.00	5.45	-126.3	-693.95
	BA	3.93	120.00	4.10	-148.27	-954.69
$ZrTe_2/HfTe_2$(Site2@Hg)	AB	3.88	120.00	6.77	-41.11	-517.77
	BA	3.88	120.00	6.07	-51.16	-648.91
$ZrTe_2/HfTe_2$(Site3@Cu)	AB	3.91	120.00	3.79	-227.08	2829.28
	BA	3.92	120.00	3.70	-248.82	1607.10
$ZrTe_2/HfTe_2$(Site3@Ag)	AB	3.91	120.00	4.49	-159.59	947.13
	BA	3.92	120.00	4.40	-168.36	880.36
$ZrTe_2/HfTe_2$(Site3@Zn)	AB	3.91	120.00	4.18	-88.81	-884.64
	BA	3.96	120.00	3.99	-93.46	-1008.07
$ZrTe_2/HfTe_2$(Site3@Au)	AB	3.90	120.00	4.41	-192.24	-603.82
	BA	3.93	120.00	4.27	-206.6	-804.06
$ZrTe_2/HfTe_2$(Site3@Hg)	AB	3.87	120.00	6.47	-43.69	-549.63
	BA	3.87	120.00	6.60	-41.6	-523.25
$CrSe_2/MoS_2$(Site1@Cu)	AB	3.18	120.00	3.58	-158.55	2305.09
	BA	3.17	120.00	4.03	-175.42	2323.85
$CrSe_2/MoS_2$(Site1@Ag)	AB	3.15	120.00	5.46	-82.39	1962.11
	BA	3.16	120.00	5.15	-93.67	1919.53

$CrSe_2/MoS_2$(Site1@Ga)	AB	3.17	120.00	5.81	-83	-458.40
	BA	3.15	120.00	5.60	-83.66	-466.76
$CrSe_2/MoS_2$(Site1@In)	AB	3.18	120.00	5.86	-79.6	-694.67
	BA	3.18	120.00	5.88	-83.97	-736.94
$CrSe_2/MoS_2$(Site1@Au)	AB	3.12	120.00	5.81	-91.38	-184.95
	BA	3.14	120.00	5.28	-103.81	-282.30
$CrSe_2/MoS_2$(Site1@Pt)	AB	3.15	120.00	4.33	-177.69	174.22
	BA	3.13	120.00	4.43	-267.04	-635.06
$CrSe_2/MoS_2$(Site2@Cu)	AB	3.19	120.00	3.95	-175.72	2321.47
	BA	3.18	120.00	3.58	-154.83	2324.36
$CrSe_2/MoS_2$(Site2@Ag)	AB	3.16	120.00	5.21	-90.9	1943.10
	BA	3.15	120.00	5.42	-82.25	1974.15
$CrSe_2/MoS_2$(Site2@Ga)	AB	3.18	120.00	5.96	-84.15	-467.55
	BA	3.17	120.00	5.79	-82.71	-455.34
$CrSe_2/MoS_2$(Site2@In)	AB	3.18	120.00	5.95	-80.84	-709.32
	BA	3.18	120.00	5.84	-79.14	-689.98
$CrSe_2/MoS_2$(Site2@Zn)	AB	3.15	120.00	5.60	-79.92	-142.97
	BA	3.16	120.00	5.59	-80.81	-153.67
$CrSe_2/MoS_2$(Site2@Au)	AB	3.13	120.00	5.46	-100.97	-259.02
	BA	3.12	120.00	5.83	-91.31	-176.89
$CrSe_2/MoS_2$(Site2@Hg)	AB	3.18	120.00	6.34	-72.07	-517.10
	BA	3.18	120.00	6.16	-78.63	-575.54
$CrSe_2/MoS_2$(Site3@Pt)	AB	3.12	120.00	4.48	-242.17	-406.70
	BA	3.15	120.00	4.39	-231.43	-306.19
$MoSe_2/CrSe_2$(Site1@Au)	AB	3.19	120.00	5.79	-95.33	-69.51
	BA	3.21	120.00	5.22	-111.06	-202.34
$MoSe_2/CrSe_2$(Site1@Pt)	AB	3.22	120.00	4.39	-208.21	116.99
	BA	3.20	120.00	4.67	-259.44	-361.48
$MoSe_2/CrSe_2$(Site2@Au)	AB	3.21	120.00	5.42	-106.53	-164.66

	BA	3.19	120.00	5.79	-94.92	-65.91
$MoSe_2/CrSe_2$(Site3@Pt)	AB	3.19	120.00	4.49	-260.88	-379.42
	BA	3.22	120.00	4.42	-252.84	-284.48
$HfS_2/HfSe_2$(Site1@Pt)	AB	3.60	120.00	3.12	-310.13	-255.43
	BA	3.72	120.00	3.24	-353.8	-567.76
$HfS_2/HfSe_2$(Site3@Pt)	AB	3.57	120.00	3.94	-298.19	-232.65
	BA	3.59	120.00	3.74	-356.01	-871.12

Table S9. AC(CA) lattice and binding energy and formation energy.

Heterostructures	Type	lattice parameter: a=b (Å)	lattice parameter: gamma (°)	Interlayer distance (Å)	Binding energy ($meV/Å^2$)	Formation energy (meV)
$MoSe_2/WSe_2$(Site3@Cu)	AC	3.26	120.00	4.26	-138.76	2460.29
	CA	3.27	120.00	4.64	-153.62	2279.75
$MoSe_2/WSe_2$(Site3@Ag)	AC	3.26	120.00	5.30	-90.44	1897.01
	CA	3.27	120.00	5.32	-97.11	1834.36
$MoSe_2/WSe_2$(Site3@Zn)	AC	3.27	120.00	5.75	-61.05	-552.17
	CA	3.26	120.00	5.80	-56.09	-493.49
$MoSe_2/WSe_2$(Site3@Au)	AC	3.25	120.00	5.36	-107.76	-153.80
	CA	3.27	120.00	5.11	-122.5	-283.84
$MoSe_2/WSe_2$(Site3@Hg)	AC	3.29	120.00	6.40	-68.14	-579.91
	CA	3.29	120.00	6.69	-60.22	-504.67
$TiS_2/TiSe_2$(Site1@Pt)	AC	3.56	120.00	3.51	-371.88	-730.89
	CA	3.44	120.00	3.59	-304.84	-353.54
$HfS_2/TiSe_2$(Site1@Pt)	AC	3.67	120.00	3.32	-359.96	-588.35
	CA	3.52	120.00	3.75	-292.62	-251.18
$MoTe_2/WTe_2$(Site1@Cu)	AC	3.53	120.00	4.20	-155.87	2017.07
	CA	3.52	120.00	4.28	-143.6	2219.44
$MoTe_2/WTe_2$(Site1@Ag)	AC	3.50	120.00	5.13	-89.89	1747.26
	CA	3.50	120.00	5.19	-88.15	1842.98
$MoTe_2/WTe_2$(Site1@Zn)	AC	3.50	120.00	6.60	-72.75	-252.53
	CA	3.51	120.00	6.57	-72.55	-252.48
$MoTe_2/WTe_2$(Site1@Au)	AC	3.49	120.00	5.11	-120.92	-22.08
	CA	3.49	120.00	5.15	-120.2	-16.85

$MoTe_2/WTe_2$(Site1@Cd)	AC	3.50	120.00	6.57	-64.57	-444.59
	CA	3.50	120.00	6.57	-64.9	-447.96
$MoTe_2/WTe_2$(Site1@Hg)	AC	3.51	120.00	6.78	-59.27	-625.28
	CA	3.51	120.00	6.77	-59.45	-626.69
$MoTe_2/WTe_2$(Site3@Pt)	AC	3.48	120.00	4.43	-320.97	-604.66
	CA	3.54	120.00	4.32	-306.73	-426.80
$TiTe_2/HfTe_2$(Site1@Cu)	AC	3.84	120.00	3.85	-233.71	1765.04
	CA	3.80	120.00	3.64	-199.46	2182.83
$TiTe_2/HfTe_2$(Site1@Au)	AC	3.83	120.00	4.46	-195.82	-620.52
	CA	3.82	120.00	4.05	-167.18	-276.66
$TiTe_2/HfTe_2$(Site1@Pt)	AC	3.96	120.00	3.79	-367.98	-908.41
	CA	3.82	120.00	3.58	-327.21	-542.85
$TiTe_2/HfTe_2$(Site3@Au)	AC	3.82	120.00	4.50	-199.03	-644.94
	CA	3.83	120.00	5.15	-226.96	-982.09
$MoSe_2/WS_2$(Site1@Ag)	AC	3.20	120.00	5.16	-90.97	2011.33
	CA	3.20	120.00	5.41	-81.42	2069.59
$MoSe_2/WS_2$(Site1@Au)	AC	3.19	120.00	5.25	-106.84	-168.18
	CA	3.18	120.00	5.69	-93.84	-52.57
$MoSe_2/WS_2$(Site1@Cd)	AC	3.21	120.00	6.08	-78.78	-475.28
	CA	3.21	120.00	6.06	-77.79	-467.15
$MoSe_2/WS_2$(Site1@Pt)	AC	3.17	120.00	4.43	-259.64	-381.34
	CA	3.22	120.00	4.21	-181.13	379.49
$MoSe_2/WS_2$(Site2@Ga)	AC	3.21	120.00	5.80	-73.03	-287.02
	CA	3.21	120.00	5.77	-75.1	-304.89
$MoSe_2/WS_2$(Site2@In)	AC	3.23	120.00	6.07	-66.99	-535.48
	CA	3.22	120.00	5.95	-68.98	-552.04
$MoSe_2/WS_2$(Site3@Ga)	AC	3.22	120.00	5.90	-80.52	-354.86
	CA	3.22	120.00	6.04	-79.49	-345.72
$MoSe_2/WS_2$(Site3@In)	AC	3.22	120.00	6.00	-73.74	-595.31

	CA	3.22	120.00	6.06	-73.11	-589.88
$ZrTe_2/TiTe_2$(Site1@Ga)	AC	3.84	120.00	5.30	-124.37	-601.34
	CA	3.84	120.00	4.37	-150.76	-932.83
$ZrTe_2/TiTe_2$(Site1@Zn)	AC	3.87	120.00	4.16	-105.99	-1007.82
	CA	3.83	120.00	3.99	-92.21	-947.75
$ZrTe_2/TiTe_2$(Site1@Au)	AC	3.85	120.00	4.46	-203.55	-675.74
	CA	3.86	120.00	4.00	-171.84	-294.71
$ZrTe_2/TiTe_2$(Site2@Cu)	AC	3.85	120.00	3.17	-240.02	1867.78
	CA	3.82	120.00	3.63	-204.94	2129.87
$ZrTe_2/TiTe_2$(Site2@Ag)	AC	3.87	120.00	3.83	-173.34	1063.09
	CA	3.85	120.00	4.10	-158.51	1137.99
$ZrTe_2/TiTe_2$(Site2@Zn)	AC	3.91	120.00	3.46	-99.74	-1019.18
	CA	3.84	120.00	3.98	-89.44	-918.73
$ZrTe_2/TiTe_2$(Site2@Au)	AC	3.90	120.00	3.66	-191.6	-521.32
	CA	3.85	120.00	3.97	-173.11	-315.54
$ZrTe_2/TiTe_2$(Site2@Hg)	AC	3.81	120.00	6.19	-52.81	-583.26
	CA	3.81	120.00	6.00	-54.99	-610.14
$ZrTe_2/TiTe_2$(Site2@Pt)	AC	3.88	120.00	3.17	-407.93	-1548.61
	CA	3.84	120.00	3.58	-335.73	-639.69
$ZrTe_2/TiTe_2$(Site3@In)	AC	3.82	120.00	6.14	-107.86	-895.09
	CA	3.80	120.00	6.55	-104.02	-844.35
$ZrTe_2/TiTe_2$(Site3@Zn)	AC	3.88	120.00	4.16	-96.2	-914.63
	CA	3.90	120.00	5.05	-72.56	-587.67
$ZrTe_2/TiTe_2$(Site3@Cd)	AC	3.89	120.00	4.89	-66.82	-690.92
	CA	3.80	120.00	5.99	-56.95	-615.26
$ZrTe_2/TiTe_2$(Site3@Hg)	AC	3.81	120.00	6.42	-47.08	-508.67
	CA	3.80	120.00	7.04	-37.04	-381.09
$ZrTe_2/TiTe_2$(Site3@Pt)	AC	3.99	120.00	3.76	-372.71	-958.45
	CA	3.77	120.00	5.04	-328.37	-491.88

$MoTe_2/CrTe_2$(Site1@Cu)	AC	3.51	120.00	4.27	-180.69	1916.54
	CA	3.50	120.00	3.91	-166.73	2059.96
$MoTe_2/CrTe_2$(Site1@Ag)	AC	3.51	120.00	5.04	-112.59	1634.44
	CA	3.50	120.00	4.72	-102.21	1638.77
$MoTe_2/CrTe_2$(Site1@Zn)	AC	3.51	120.00	5.16	-50.14	2.66
	CA	3.52	120.00	4.62	-62.28	-131.47
$MoTe_2/CrTe_2$(Site1@Au)	AC	3.51	120.00	4.93	-150.7	-310.66
	CA	3.50	120.00	4.69	-126.12	-66.78
$MoTe_2/CrTe_2$(Site1@Hg)	AC	3.50	120.00	6.68	-61.62	-628.76
	CA	3.50	120.00	6.40	-68.8	-715.97
$MoTe_2/CrTe_2$(Site1@Pt)	AC	3.49	120.00	4.51	-323.84	-630.44
	CA	3.52	120.00	4.15	-292.76	-269.88
HfS_2/ZrS_2(Site1@Au)	AC	3.54	120.00	4.15	-181.02	-547.64
	CA	3.55	120.00	3.70	-145.28	-177.48
HfS_2/ZrS_2(Site1@Cd)	AC	3.51	120.00	5.57	-90.77	-697.38
	CA	3.56	120.00	3.87	-102.63	-716.45
HfS_2/ZrS_2(Site2@Cu)	AC	3.51	120.00	2.84	-289.19	1756.76
	CA	3.51	120.00	3.22	-244.87	2514.05
HfS_2/ZrS_2(Site2@Ag)	AC	3.55	120.00	3.60	-187.08	1102.55
	CA	3.54	120.00	3.71	-178.11	1105.72
HfS_2/ZrS_2(Site2@Zn)	AC	3.55	120.00	2.97	-166.63	-1092.87
	CA	3.52	120.00	3.34	-135.84	-707.45
HfS_2/ZrS_2(Site2@Au)	AC	3.56	120.00	3.46	-154.07	-264.61
	CA	3.56	120.00	3.65	-144.31	-158.38
HfS_2/ZrS_2(Site2@Cd)	AC	3.60	120.00	3.58	-114.5	-822.32
	CA	3.57	120.00	3.84	-104.91	-726.77
HfS_2/ZrS_2(Site2@Pt)	AC	3.53	120.00	2.93	-371.03	-1070.80
	CA	3.52	120.00	3.58	-294.19	-280.88
$ZrS_2/ZrSe_2$(Site1@Pt)	AC	3.77	120.00	3.15	-381.88	-910.49

	CA	3.64	120.00	3.49	-293.16	-144.29
WS_2/WSe_2(Site2@Pt)	AC	3.17	120.00	4.76	-153.55	537.88
	CA	3.22	120.00	4.24	-180.42	375.79
WS_2/WSe_2(Site3@Cu)	AC	3.19	120.00	4.19	-137.72	2648.64
	CA	3.20	120.00	4.55	-152.39	2481.98
WS_2/WSe_2(Site3@Zn)	AC	3.21	120.00	5.70	-68.25	-478.39
	CA	3.20	120.00	5.79	-64.05	-432.15
WS_2/WSe_2(Site3@Au)	AC	3.19	120.00	5.28	-108.06	-177.11
	CA	3.20	120.00	5.08	-118.68	-286.78
WS_2/WSe_2(Site3@Hg)	AC	3.23	120.00	6.39	-69.4	-478.74
	CA	3.23	120.00	6.64	-61.49	-403.82
$HfSe_2/ZrSe_2$(Site1@Au)	AC	3.67	120.00	4.30	-169.23	-374.70
	CA	3.69	120.00	3.80	-146.47	-120.89
$HfSe_2/ZrSe_2$(Site1@Cd)	AC	3.64	120.00	5.79	-70.47	-743.52
	CA	3.70	120.00	4.10	-77.75	-815.46
$HfSe_2/ZrSe_2$(Site2@Cu)	AC	3.66	120.00	2.97	-253.15	1843.01
	CA	3.65	120.00	3.36	-214.39	2749.00
$HfSe_2/ZrSe_2$(Site2@Zn)	AC	3.70	120.00	3.13	-122.7	-769.72
	CA	3.66	120.00	3.58	-100.51	-489.00
$HfSe_2/ZrSe_2$(Site2@Au)	AC	3.71	120.00	3.55	-157.94	-236.90
	CA	3.69	120.00	3.79	-143.64	-87.77
$HfSe_2/ZrSe_2$(Site2@Cd)	AC	3.74	120.00	3.78	-83.9	-855.12
	CA	3.70	120.00	4.09	-78.6	-823.52
$HfSe_2/ZrSe_2$(Site2@Pt)	AC	3.69	120.00	3.06	-355.12	-908.75
	CA	3.68	120.00	3.64	-284.77	-83.52
$WS_2/CrSe_2$(Site1@Cu)	AC	3.15	120.00	4.21	-142.2	2540.17
	CA	3.17	120.00	3.83	-126.4	2487.62
$WS_2/CrSe_2$(Site1@Ag)	AC	3.15	120.00	5.31	-90.44	1938.25
	CA	3.15	120.00	5.50	-82.02	1966.24

$WS_2/CrSe_2$(Site1@Hg)	AC	3.18	120.00	6.29	-73.16	-526.93
	CA	3.19	120.00	6.17	-77.97	-571.43
$WS_2/CrSe_2$(Site2@Ag)	AC	3.14	120.00	5.83	-80.56	1979.76
	CA	3.15	120.00	5.53	-82.08	1976.84
$WS_2/CrSe_2$(Site2@Pt)	AC	3.14	120.00	4.74	-175.34	164.62
	CA	3.12	120.00	4.67	-179.27	103.11
$HfSe_2/TiSe_2$(Site2@Cu)	AC	3.58	120.00	3.06	-258.89	1872.34
	CA	3.56	120.00	3.40	-224.36	2095.84
$HfSe_2/TiSe_2$(Site2@Au)	AC	3.62	120.00	3.71	-157.88	-197.08
	CA	3.60	120.00	3.89	-148	-102.70
$HfSe_2/TiSe_2$(Site2@Pt)	AC	3.62	120.00	3.14	-361.35	-887.76
	CA	3.59	120.00	3.58	-292.33	-150.23
$ZrS_2/HfSe_2$(Site1@Pt)	AC	3.74	120.00	3.23	-370.9	-833.28
	CA	3.62	120.00	3.51	-282.44	-55.20
$CrSe_2/WSe_2$(Site3@Au)	AC	3.21	120.00	5.30	-112.37	-217.68
	CA	3.23	120.00	5.07	-131	-373.31
WS_2/MoS_2(Site1@Cu)	AC	3.13	120.00	4.09	-147.7	2581.38
	CA	3.15	120.00	3.72	-131.43	2513.75
WS_2/MoS_2(Site1@Zn)	AC	3.15	120.00	5.49	-77.19	-116.94
	CA	3.15	120.00	5.52	-76.82	-118.00
WS_2/MoS_2(Site1@Au)	AC	3.13	120.00	5.31	-102.22	-276.69
	CA	3.12	120.00	5.70	-90.54	-176.47
WS_2/MoS_2(Site1@Hg)	AC	3.17	120.00	6.22	-71.24	-502.93
	CA	3.18	120.00	6.06	-76.76	-551.88
WS_2/MoS_2(Site1@Pt)	AC	3.11	120.00	4.38	-247.41	-475.60
	CA	3.14	120.00	4.35	-168.9	231.85
WS_2/MoS_2(Site2@Pt)	AC	3.15	120.00	4.53	-161.66	297.62
	CA	3.12	120.00	4.40	-151.26	336.69
$CrTe_2/WTe_2$(Site1@Au)	AC	3.50	120.00	5.01	-129.21	-103.68

	CA	3.51	120.00	5.09	-131.33	-111.12
$CrTe_2/WTe_2$(Site1@Hg)	AC	3.50	120.00	6.82	-60.25	-624.18
	CA	3.50	120.00	6.75	-61.16	-632.55
$CrTe_2/WTe_2$(Site3@Au)	AC	3.51	120.00	4.93	-149.03	-284.95
	CA	3.50	120.00	5.10	-131.24	-111.15
CrS_2/MoS_2(Site2@Au)	AC	3.05	120.00	5.84	-86.41	-156.62
	CA	3.05	120.00	5.77	-88.71	-175.19
CrS_2/MoS_2(Site3@Au)	AC	3.07	120.00	5.19	-104.54	-299.06
	CA	3.11	120.00	4.78	-138.83	-537.08
$ZrS_2/TiSe_2$(Site1@Pt)	AC	3.69	120.00	3.29	-381.6	-857.41
	CA	3.55	120.00	3.64	-301.13	-298.90
$MoSe_2/MoS_2$(Site1@Hg)	AC	3.23	120.00	6.29	-70.77	-489.00
	CA	3.23	120.00	6.10	-76.31	-541.10
$ZrTe_2/HfTe_2$(Site1@Cu)	AC	3.92	120.00	3.75	-232.35	2778.19
	CA	3.88	120.00	3.64	-193.9	3264.86
$ZrTe_2/HfTe_2$(Site1@Ag)	AC	3.91	120.00	4.45	-162.04	1000.21
	CA	3.90	120.00	4.07	-148.66	1162.68
$ZrTe_2/HfTe_2$(Site1@Au)	AC	3.91	120.00	4.37	-192.47	-605.38
	CA	3.90	120.00	3.95	-162.61	-241.60
$ZrTe_2/HfTe_2$(Site1@Pt)	AC	4.09	120.00	3.54	-367.99	-950.25
	CA	3.90	120.00	3.70	-315.61	-452.64
$ZrTe_2/HfTe_2$(Site2@Hg)	AC	3.88	120.00	6.20	-49.42	-627.39
	CA	3.88	120.00	6.03	-51.7	-657.30
$ZrTe_2/HfTe_2$(Site3@Au)	AC	3.90	120.00	4.41	-189	-565.47
	CA	3.91	120.00	5.15	-216.65	-906.47
$ZrTe_2/HfTe_2$(Site3@Hg)	AC	3.87	120.00	6.50	-43.67	-549.35
	CA	3.87	120.00	7.21	-33.07	-411.89
$CrSe_2/MoS_2$(Site1@Cu)	AC	3.17	120.00	4.04	-174.39	2331.95
	CA	3.17	120.00	3.69	-152.8	2329.37

$CrSe_2/MoS_2$(Site1@Ag)	AC	3.16	120.00	5.15	-94.19	1914.07
	CA	3.15	120.00	5.44	-82.63	1960.11
$CrSe_2/MoS_2$(Site1@Ga)	AC	3.16	120.00	5.67	-82.46	-457.18
	CA	3.18	120.00	5.79	-82.76	-457.10
$CrSe_2/MoS_2$(Site1@In)	AC	3.18	120.00	5.90	-82.85	-727.31
	CA	3.18	120.00	5.87	-78.93	-689.00
$CrSe_2/MoS_2$(Site1@Au)	AC	3.14	120.00	5.25	-104.96	-292.31
	CA	3.12	120.00	5.80	-91.65	-187.34
$CrSe_2/MoS_2$(Site1@Pt)	AC	3.12	120.00	4.45	-268.14	-648.85
	CA	3.16	120.00	4.32	-179.34	175.97
$CrSe_2/MoS_2$(Site2@Zn)	AC	3.16	120.00	5.62	-80.48	-150.92
	CA	3.16	120.00	5.51	-82.43	-167.36
$CrSe_2/MoS_2$(Site2@Hg)	AC	3.19	120.00	6.17	-77.31	-564.81
	CA	3.18	120.00	6.14	-79.06	-578.98
$CrSe_2/MoS_2$(Site3@Ga)	AC	3.19	120.00	5.95	-88.86	-494.27
	CA	3.15	120.00	5.65	-86.25	-489.97
$CrSe_2/MoS_2$(Site3@In)	AC	3.19	120.00	5.92	-84.65	-739.26
	CA	3.19	120.00	5.99	-85.1	-742.75
$CrSe_2/MoS_2$(Site3@Zn)	AC	3.15	120.00	5.47	-83.46	-172.84
	CA	3.15	120.00	5.28	-86.62	-197.13
$CrSe_2/MoS_2$(Site3@Hg)	AC	3.18	120.00	6.24	-74.2	-535.46
	CA	3.18	120.00	6.47	-67.16	-472.38
$MoSe_2/CrSe_2$(Site1@Au)	AC	3.21	120.00	5.18	-112.2	-211.73
	CA	3.19	120.00	5.78	-95.58	-71.74
$MoSe_2/CrSe_2$(Site1@Pt)	AC	3.20	120.00	4.68	-260.1	-370.14
	CA	3.22	120.00	4.40	-208.1	121.97
$MoSe_2/CrSe_2$(Site2@Au)	AC	3.19	120.00	5.88	-92.71	-45.68
	CA	3.19	120.00	5.79	-95.21	-68.33
$MoSe_2/CrSe_2$(Site2@Pt)	AC	3.22	120.00	4.62	-198.4	209.39

	CA	3.19	120.00	4.57	-195.12	193.42
$HfS_2/HfSe_2$(Site1@Pt)	AC	3.73	120.00	3.23	-354.01	-546.76
	CA	3.59	120.00	3.63	-274.24	8.86

Table S10. Summary of five-number statistics: minimum (min), first quartile (Q1), median (med), third quartile (Q3) and maximum (max) for each structural group shown in the violin plots. The left panel of Figure 6 corresponds to the interlayer distance distributions of AB(BA) and AC(CA) stacking configurations; the right panel shows the corresponding binding energy distributions.

	Interlayer Distance (Å)				Binding Energy (meV · Å^2)			
	AB	BA	AC	CA	AB	BA	AC	CA
min	2.95	2.92	2.84	3.09	-539.02	-537.93	-537.36	-416.78
Q1	3.99	4.04	4.09	4.08	-170.49	-171.35	-167.52	-161.18
med	4.91	4.87	4.84	4.88	-115.32	-116.07	-114.56	-113.75
Q3	5.88	5.88	5.89	5.86	-79.13	-79.13	-78.68	-79.18
max	6.98	7.16	6.82	7.21	-19.51	-19.98	-21.13	-14.92

Table S11. DFT total energies of four representative metal-intercalated TMD heterobilayers constructed with 2H and 1T host phases, E_{2H} and E_{1T}, and their energy differences $\Delta E = E_{1T} - E_{2H}$ (in eV per 1×1 bilayer cell). All values are given in eV.

	E (2H-Phase)	**E (1T-Phase)**	$\Delta E = E_{1T} - E_{2H}$
HfS_2/ZrS_2(Site1@Pt)	−49.95	−48.09	+1.86
$ZrS_2/HfSe_2$(Site1@Pt)	−49.27	−48.48	+0.79
WS_2/MoS_2(Site2@Pt)	−51.57	−49.64	+1.93
$CrTe_2/WTe_2$(Site1@Au)	−40.02	−40.10	−0.08

Table S12. Sliding energy barriers (E_{bar}, in meV/f.u.) of all AB(BA)-type heterostructures calculated using the CI-NEB method.

	Structure (Site@Intercalated Metal)	E_{bar}
1	$CrSe_2/MoS_2$(Site1@Ag)	0.1
2	$CrSe_2/MoS_2$(Site2@Zn)	0.4
3	WS_2/MoS_2(Site1@Zn)	0.5
4	$ZrTe_2/HfTe_2$(Site1@Au)	0.7
5	$MoSe_2/WS_2$(Site2@Zn)	0.9
6	$MoTe_2/WTe_2$(Site3@Ag)	1.0
7	WS_2/MoS_2(Site1@Au)	1.0
8	$CrSe_2/MoS_2$(Site1@Pt)	1.2
9	$MoSe_2/WS_2$(Site1@Cd)	1.9
10	$CrSe_2/MoS_2$(Site2@Cu)	2.0
11	$ZrTe_2/HfTe_2$(Site3@Ag)	2.4
12	$MoSe_2/WS_2$(Site2@Cd)	2.5
13	$MoSe_2/WS_2$(Site1@Ag)	2.6
14	$CrSe_2/MoS_2$(Site1@Cu)	4.0
15	$ZrTe_2/TiTe_2$(Site2@Cd)	7.4
16	$CrSe_2/MoS_2$(Site2@Ga)	9.0
17	$MoTe_2/CrTe_2$(Site1@Zn)	9.4
18	$CrSe_2/MoS_2$(Site2@In)	15.2
19	$MoSe_2/WS_2$(Site2@Ga)	20.5
20	$TiTe_2/HfTe_2$(Site3@Zn)	24.0
21	$HfS_2/TiSe_2$(Site3@Cu)	27.1
22	$WS_2/CrSe_2$(Site1@Hg)	41.6
23	WS_2/MoS_2(Site1@Hg)	47.0
24	HfS_2/ZrS_2(Site1@Hg)	47.8
25	$MoSe_2/MoS_2$(Site1@Hg)	51.6
26	$MoTe_2/CrTe_2$(Site1@Pt)	56.6
27	$MoTe_2/CrTe_2$(Site1@Cu)	64.3
28	$MoTe_2/WTe_2$(Site3@Pt)	65.4
29	$ZrTe_2/HfTe_2$(Site3@Cu)	69.4
30	$MoTe_2/CrTe_2$(Site1@Hg)	80.8
31	$HfSe_2/ZrSe_2$(Site2@Ag)	83.0
32	$ZrTe_2/HfTe_2$(Site1@Cu)	122.8
33	HfS_2/ZrS_2(Site2@Ag)	127.5
34	$ZrTe_2/TiTe_2$(Site2@Zn)	132.9
35	$HfSe_2/TiTe_2$(Site3@Pt)	313.2
36	$ZrTe_2/HfTe_2$(Site1@Pt)	378.7
37	$ZrTe_2/TiTe_2$(Site1@Pt)	398.6
38	$ZrTe_2/TiTe_2$(Site1@Ga)	459.5
39	$MoSe_2/CrSe_2$(Site3@Pt)	595.6

40	$HfS_2/TiSe_2$(Site3@Pt)	902.1
41	$ZrS_2/HfSe_2$(Site1@Pt)	1082.1

Table S13. Sliding energy barriers (E_{bar}, in meV/f.u.) of all AC(CA)-type heterostructures calculated using the CI-NEB method.

	Structure (Site@Intercalated Metal)	E_{bar}
1	$MoSe_2/WS_2$(Site2@In)	0.3
2	$CrSe_2/MoS_2$(Site3@Zn)	0.5
3	$CrSe_2/MoS_2$(Site1@Cu)	0.9
4	$CrSe_2/MoS_2$(Site2@Zn)	1.0
5	WS_2/MoS_2(Site1@Zn)	1.1
6	$ZrTe_2/TiTe_2$(Site2@Cu)	1.1
7	$ZrS_2/TiSe_2$(Site1@Pt)	1.4
8	$CrSe_2/MoS_2$(Site2@Hg)	6.2
9	$MoSe_2/WS_2$(Site3@In)	6.2
10	$MoSe_2/WS_2$(Site3@Ga)	10.0
11	$MoSe_2/WS_2$(Site1@Cd)	10.1
12	$HfS_2/TiSe_2$(Site1@Pt)	14.2
13	$CrSe_2/MoS_2$(Site3@Ga)	14.5
14	$ZrTe_2/TiTe_2$(Site2@Hg)	16.1
15	$ZrTe_2/HfTe_2$(Site2@Hg)	17.9
16	$CrSe_2/WSe_2$(Site3@Au)	34.3
17	$HfSe_2/ZrSe_2$(Site2@Cd)	44.1
18	$MoTe_2/WTe_2$(Site1@Au)	46.1
19	$ZrTe_2/TiTe_2$(Site1@Zn)	58.9
20	$MoTe_2/CrTe_2$(Site1@Ag)	94.9
21	$ZrTe_2/TiTe_2$(Site2@Zn)	100.6
22	$MoTe_2/CrTe_2$(Site1@Cu)	117.0
23	$TiTe_2/HfTe_2$(Site1@Au)	126.4
24	$MoTe_2/WTe_2$(Site1@Cu)	130.1
25	WS_2/WSe_2(Site3@Au)	139.2
26	CrS_2/MoS_2(Site3@Au)	147.5
27	$ZrTe_2/HfTe_2$(Site1@Ag)	157.9
28	$HfSe_2/TiSe_2$(Site2@Cu)	171.3
29	$MoTe_2/WTe_2$(Site3@Pt)	185.1
30	$ZrTe_2/TiTe_2$(Site2@Ag)	187.6
31	$HfSe_2/ZrSe_2$(Site2@Zn)	278.7
32	$ZrTe_2/TiTe_2$(Site3@Zn)	345.8
33	$MoTe_2/CrTe_2$(Site1@Pt)	380.3
34	$HfSe_2/ZrSe_2$(Site2@Cu)	460.3
35	$ZrTe_2/TiTe_2$(Site3@Pt)	639.5
36	$ZrTe_2/TiTe_2$(Site2@Pt)	948.2
37	$TiTe_2/HfTe_2$(Site1@Cu)	1136.0
38	$ZrTe_2/HfTe_2$(Site3@Au)	1299.1
39	$MoSe_2/WSe_2$(Site3@Ag)	1942.5

40	HfS_2/ZrS_2(Site2@Pt)	2183.1

Table S14. Ten-fold cross-validation results, including the coefficient of determination (R^2), mean absolute error (MAE), and root mean square error (RMSE) for each fold. The best performance was observed in fold 3.

Fold	R^2	MAE	RMSE
1	0.9794	0.0051	0.0073
2	0.9839	0.0047	0.0065
3	0.9872	0.0046	0.0061
4	0.9809	0.0051	0.0071
5	0.9720	0.0062	0.0083
6	0.9760	0.0060	0.0080
7	0.9779	0.0051	0.0072
8	0.9822	0.0050	0.0067
9	0.9825	0.0052	0.0070
10	0.9793	0.0050	0.0068
Mean	0.9801	0.0052	0.0071

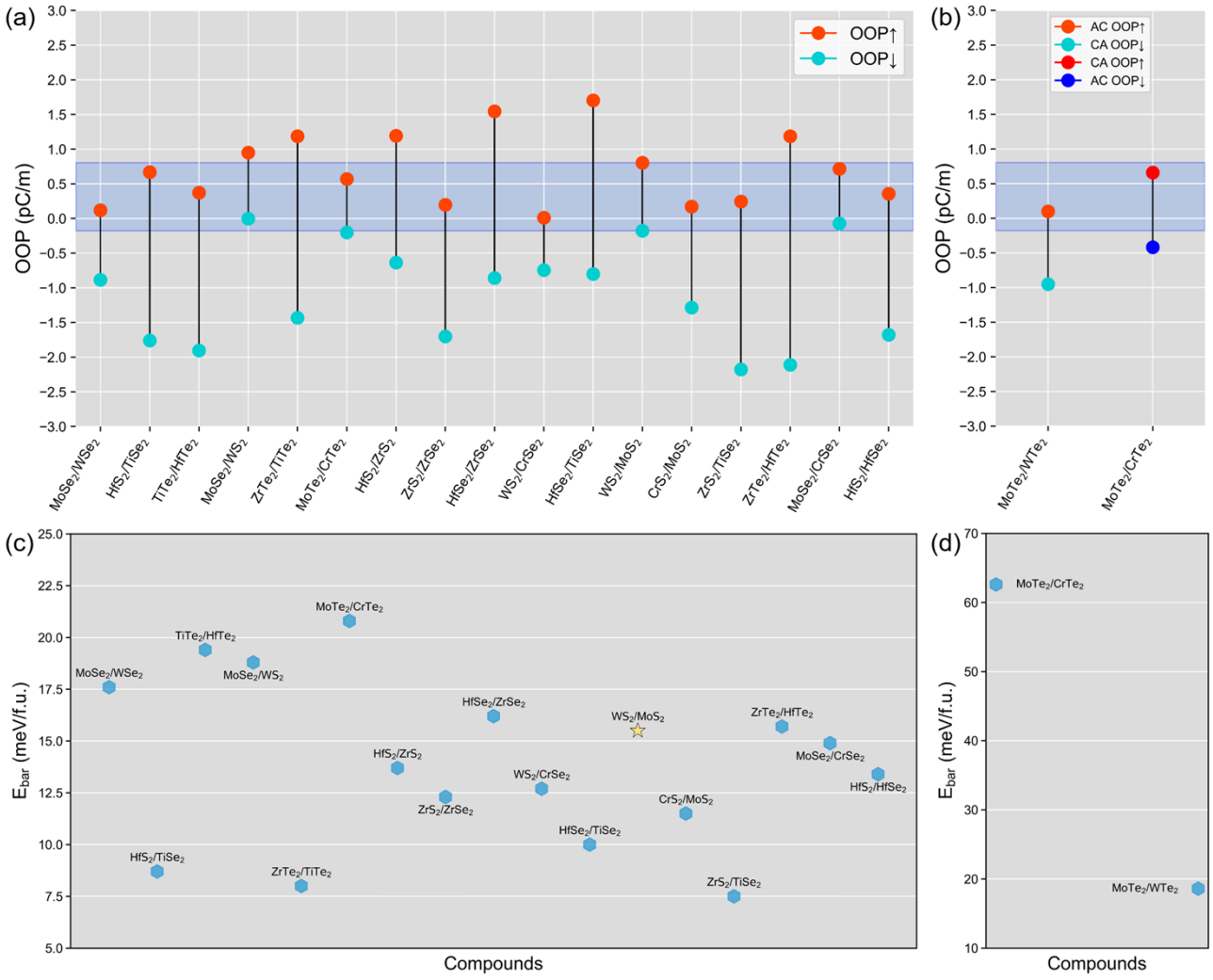

Figure S1. (a) Out-of-plane polarization (OOP) distribution of (a) sixteen AB(BA)-stacked and (b) two AC(CA)-stacked heterobilayers that exhibit sliding ferroelectricity. The experimentally reported reference system WS_2/MoS_2 is also included for comparison. Orange Red dots represent positive OOP↑, Dark Turquoise dots indicate negative OOP↓, and the shaded blue region denotes the OOP range of the reference WS_2/MoS_2 structure. Sliding energy barriers for the (c) AB(BA)- and (d) AC(CA)-stacked structures. Hexagonal markers represent the bilayers with confirmed sliding ferroelectricity, while the pentagram denotes the experimental reference WS_2/MoS_2.

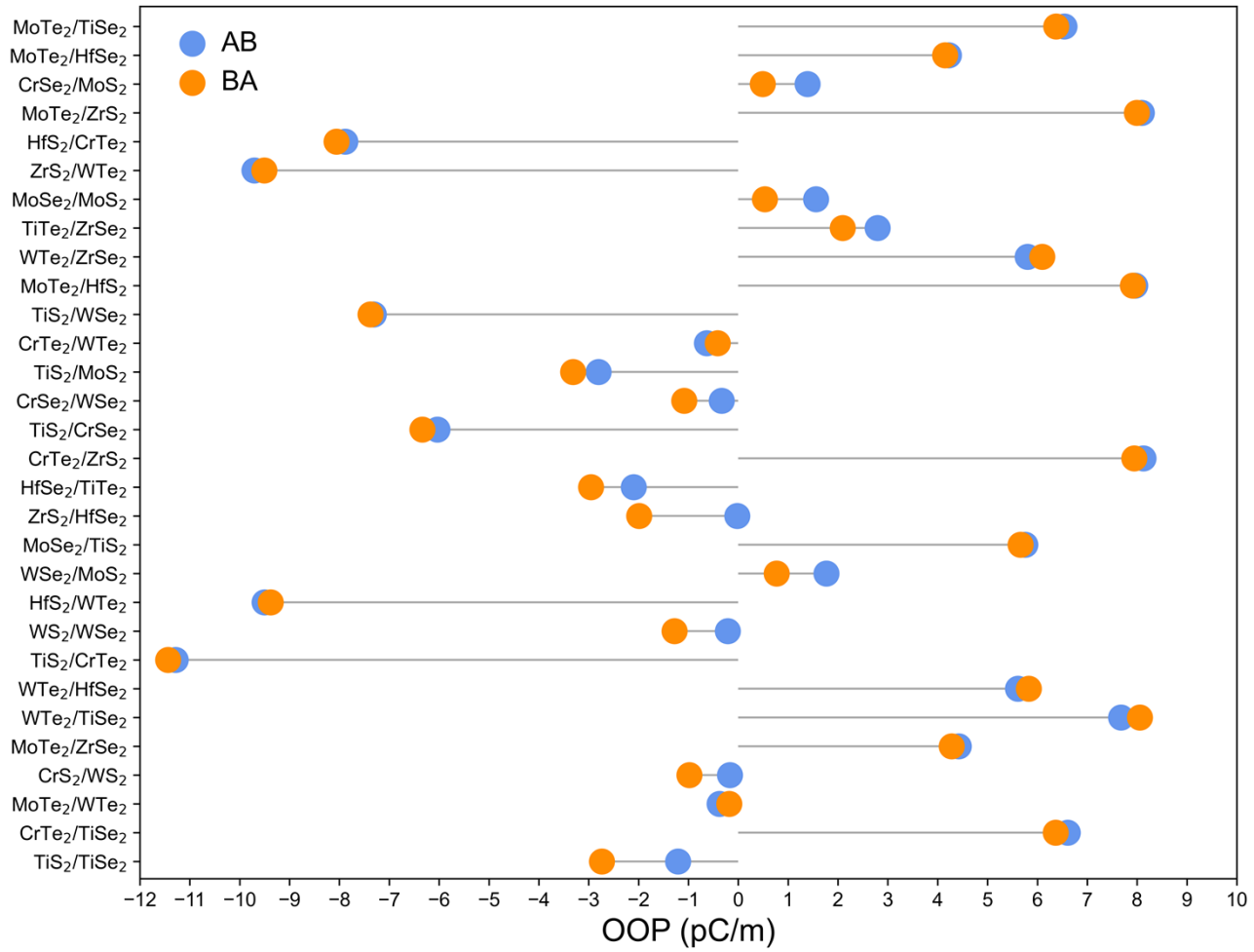

Figure S2. Out-of-plane polarization (OOP) distribution of the remaining 30 AB(BA) stacked heterobilayers (out of 47) that do not exhibit sliding ferroelectric behavior. The Y-axis indicates the structure identity, and the X-axis represents the OOP value. CornflowerBlue points denote AB-stacked structures, while DarkOrange points represent BA-stacked structures. It can be observed that the OOP directions of all pairs are the same (either both positive or both negative), indicating the absence of polarization reversibility, which is a necessary condition for sliding ferroelectricity.

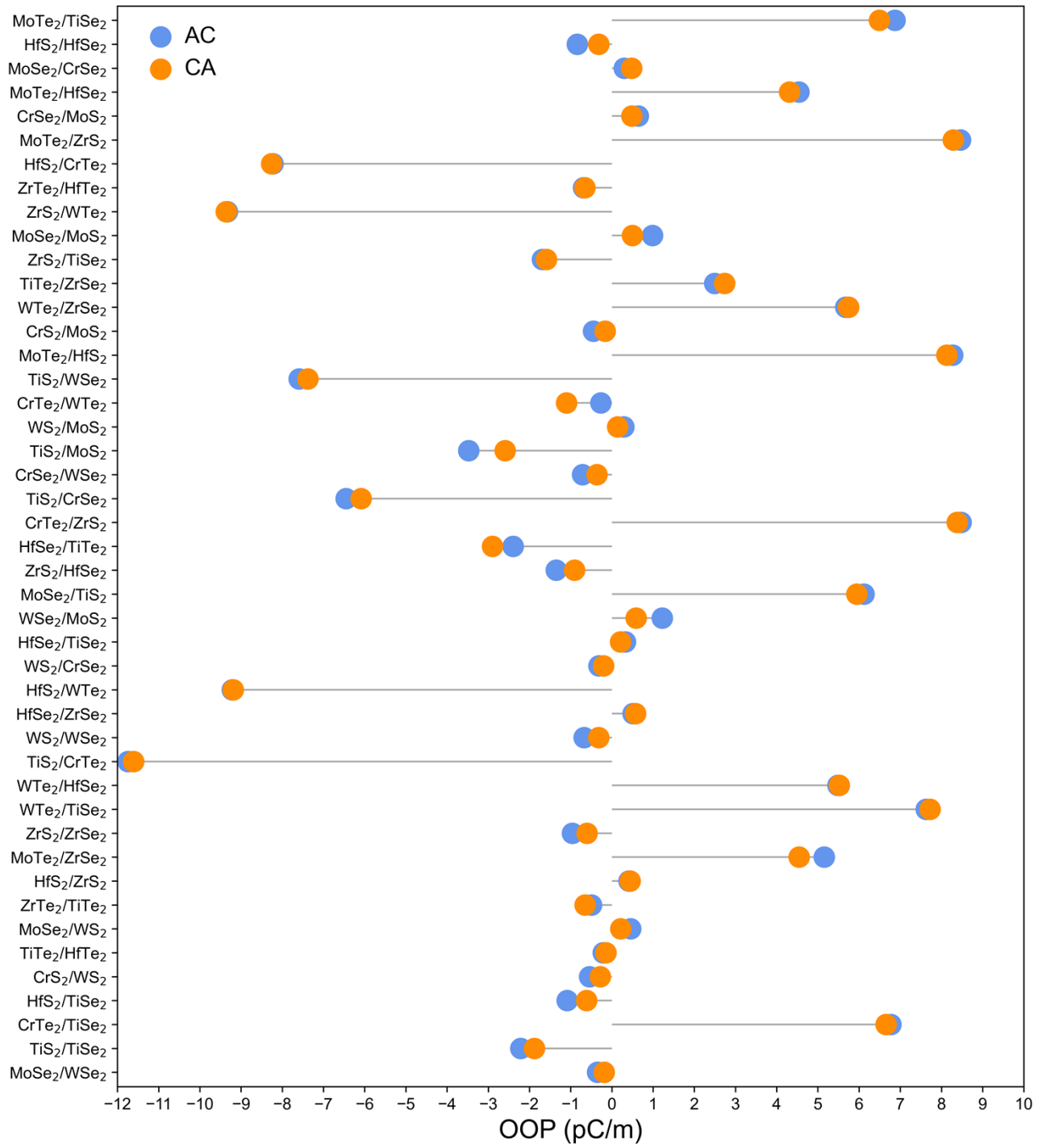

Figure S3. Out-of-plane polarization (OOP) distribution of the remaining 45 AC(CA) stacked heterobilayers (out of 47) that do not exhibit sliding ferroelectric behavior. The Y-axis indicates the structure identity, and the X-axis represents the OOP value. CornflowerBlue points denote AC-stacked structures, while DarkOrange points represent CA-stacked structures. It can be observed that the OOP directions of all pairs are the same (either both positive or both negative), indicating the absence of polarization reversibility, which is a necessary condition for sliding ferroelectricity.

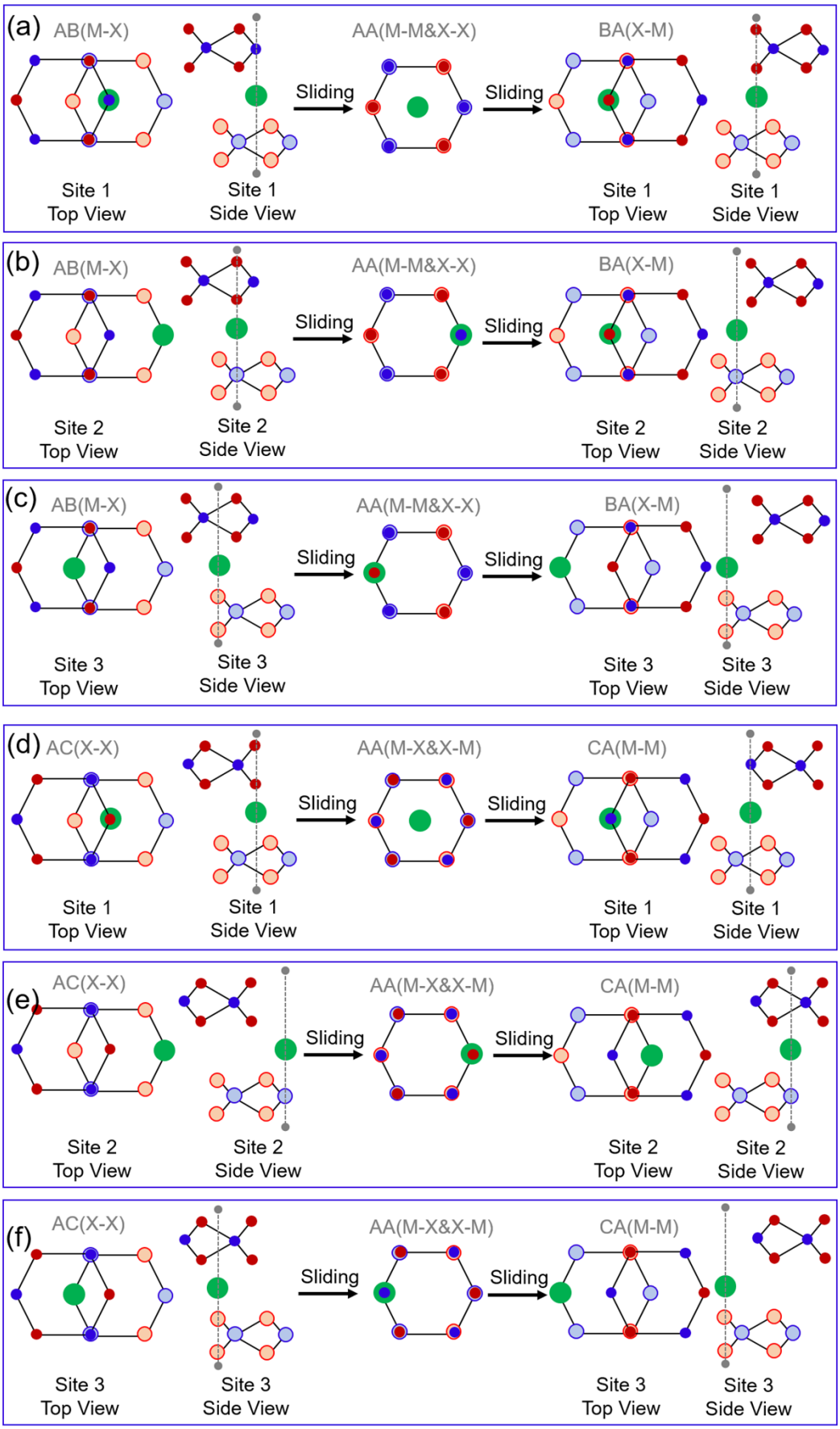

Figure S4. Schematic illustration of the three intercalation sites in different stacking sequences

(AB/BA and AC/CA). Panels (a–c) show the three sites (Site1,Site2 and Site3) along the AB–AA–BA sliding pathway: the left column displays the top and side views of the AB stacking, with green spheres denoting the intercalated atoms and gray dashed lines indicating their positions relative to the top and bottom M/X atoms; the middle column shows the top view of the intermediate AA stacking obtained by sliding the top layer to the right; the right column presents the top and side views of the BA stacking, using the same color and line conventions. Panels (d–f) depict the corresponding three sites (Site1, Site2 and Site3) along the AC–AA–CA sliding pathway, with the same layout and notation as in (a–c).

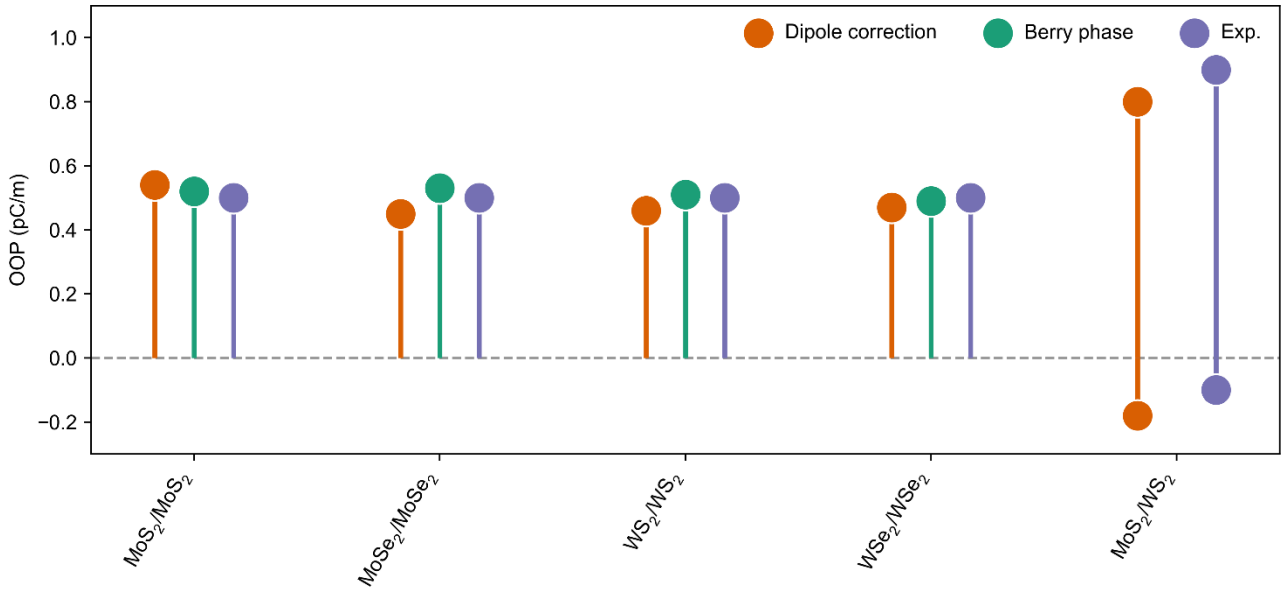

Figure S5. Out-of-plane polarization values of representative TMD bilayer systems calculated using the dipole correction method, together with Berry-phase results and available experimental values. For each structure, the OOP values obtained from different approaches are shown using a lollipop representation, with different colors indicating different methods. For the MoS_2/WS_2 heterobilayer, both positive and negative OOP components are displayed.

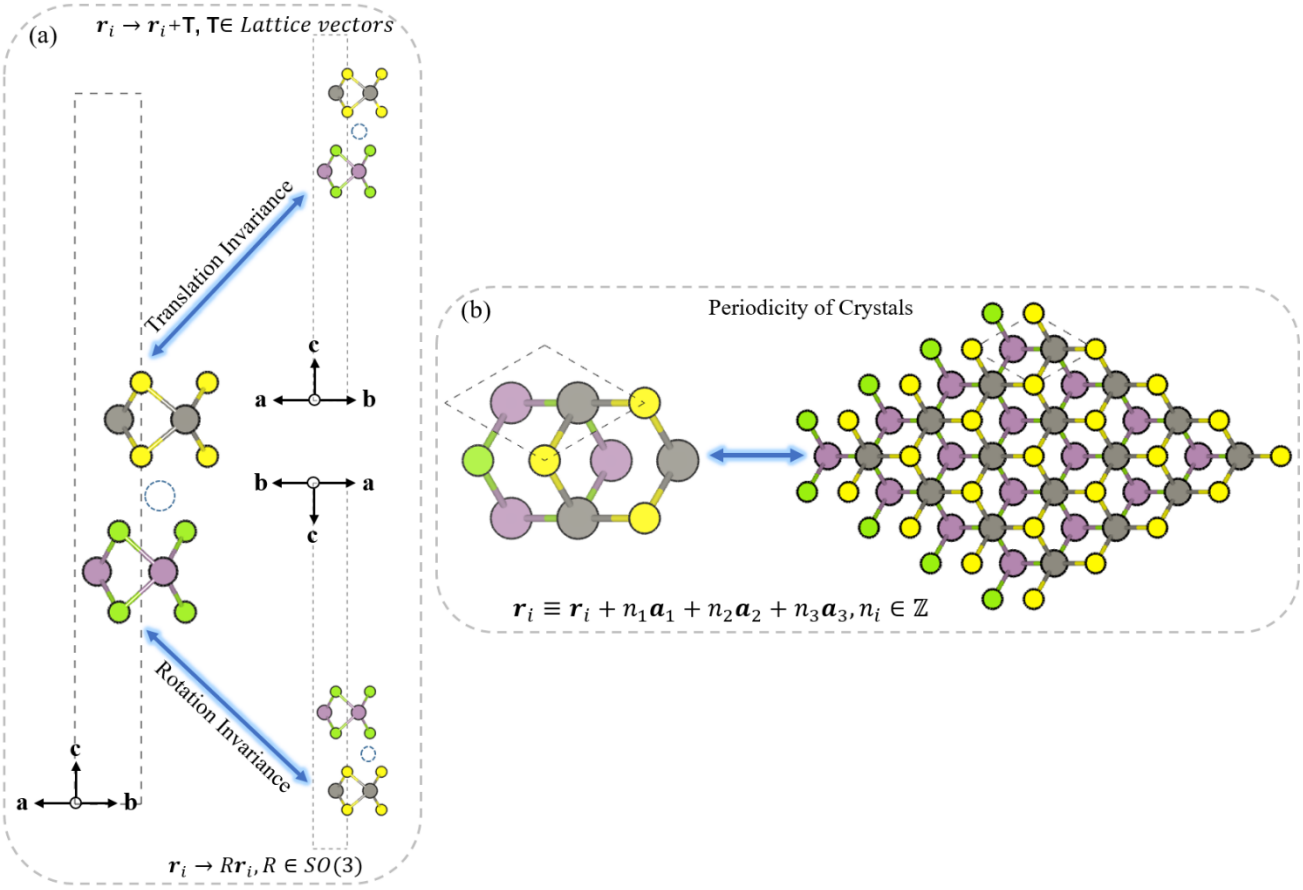

Figure S6. (a) Illustrates of the translational ($^{r_i \rightarrow r_i}$+**T, T** $\in Lattice\ vectors$, where ^{r_i} is the Cartesian coordinate of atom i, and **T** is a lattice translation vector.) and rotational ($^{r_i \rightarrow Rr_i, R \in SO(3)}$, where $R \in SO(3)$ is a 3D rotation matrix and ^{r_i} is the position atom i.) invariance and periodicity of crystals. (b) shows that the physical properties ($^{r_i \equiv r_i + n_1a_1 + n_2a_2 + n_3a_3, n_i \in Z}$, where $^{a_1, a_2, a_3}$ are the lattice basis vectors, and $^{n_1, n_2, n_3 \in Z}$) of the crystal remain consistent between the unit cell and the corresponding supercell. In the figures, gold and green atoms represent chalcogen elements (S, Se, Te), gray and purple atoms denote metal elements (Cr, Mo, Hf, Ti, Zr, W), and dashed atoms indicate intercalated atoms.

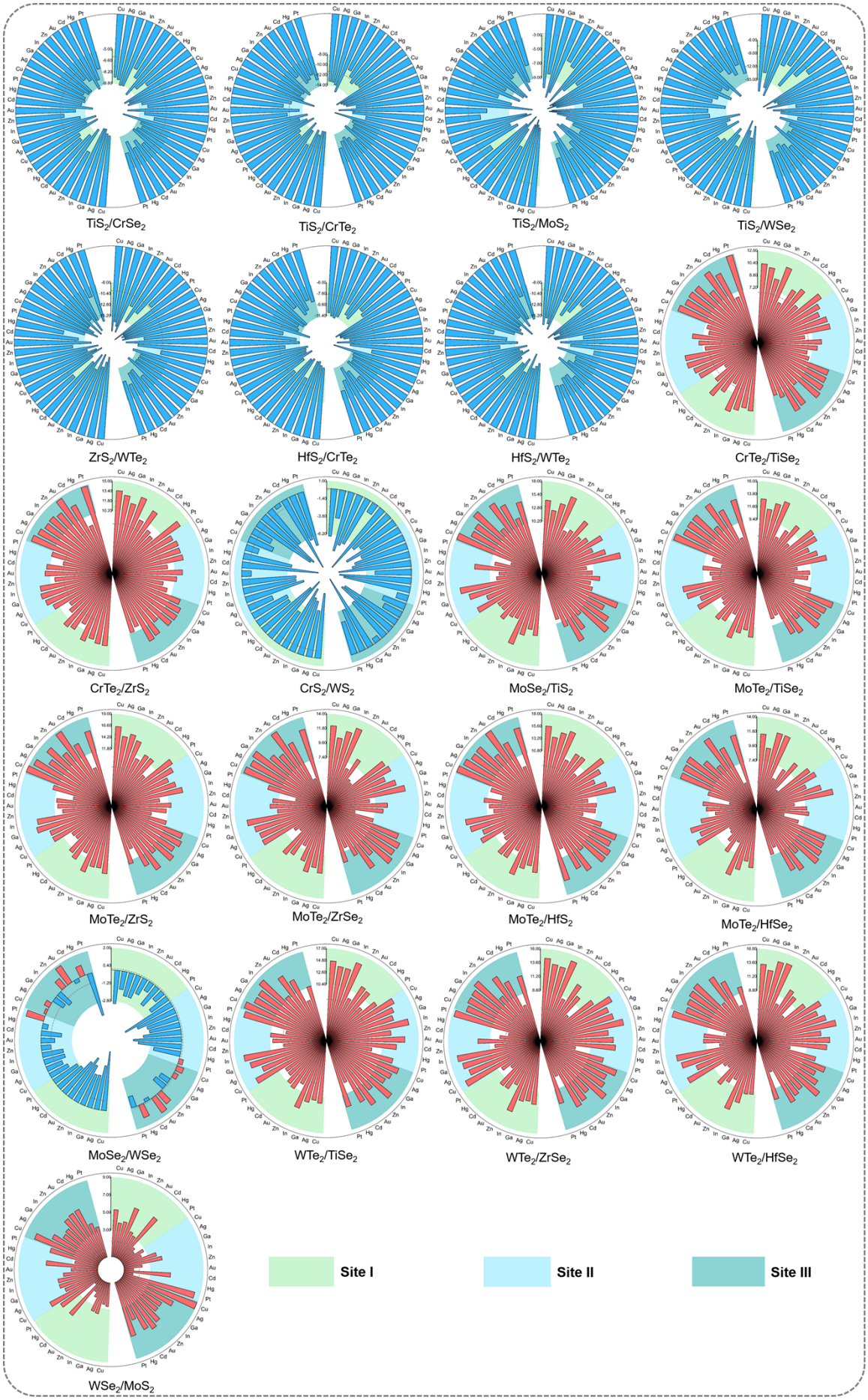
TiS2/CrSe2
TiS2/CrTe2
TiS2/MoS2
TiS2/WSe2
ZrS2/WTe2
HfS2/CrTe2
HfS2/WTe2
CrTe2/TiSe2
CrTe2/ZrS2
CrS2/WS2
MoSe2/TiS2
MoTe2/TiSe2
MoTe2/ZrS2
MoTe2/ZrSe2
MoTe2/HfS2
MoTe2/HfSe2
MoSe2/WSe2
WTe2/TiSe2
WTe2/ZrSe2
WTe2/HfSe2
WSe2/MoS2
Site I
Site II
Site III

Figure S7. Radial bar plots of out-of-plane polarization for the remaining 21 AB(BA) heterobilayers that do not exhibit switchable out-of-plane polarization. In these structures, both stacking configurations show polarization in the same direction, indicating the absence of sliding ferroelectric behavior. The visualization follows the same convention as in the main text: red and blue bars represent positive and negative polarization values, respectively, while background colors distinguish the intercalation sites. All OOP values are reported in pC/m.

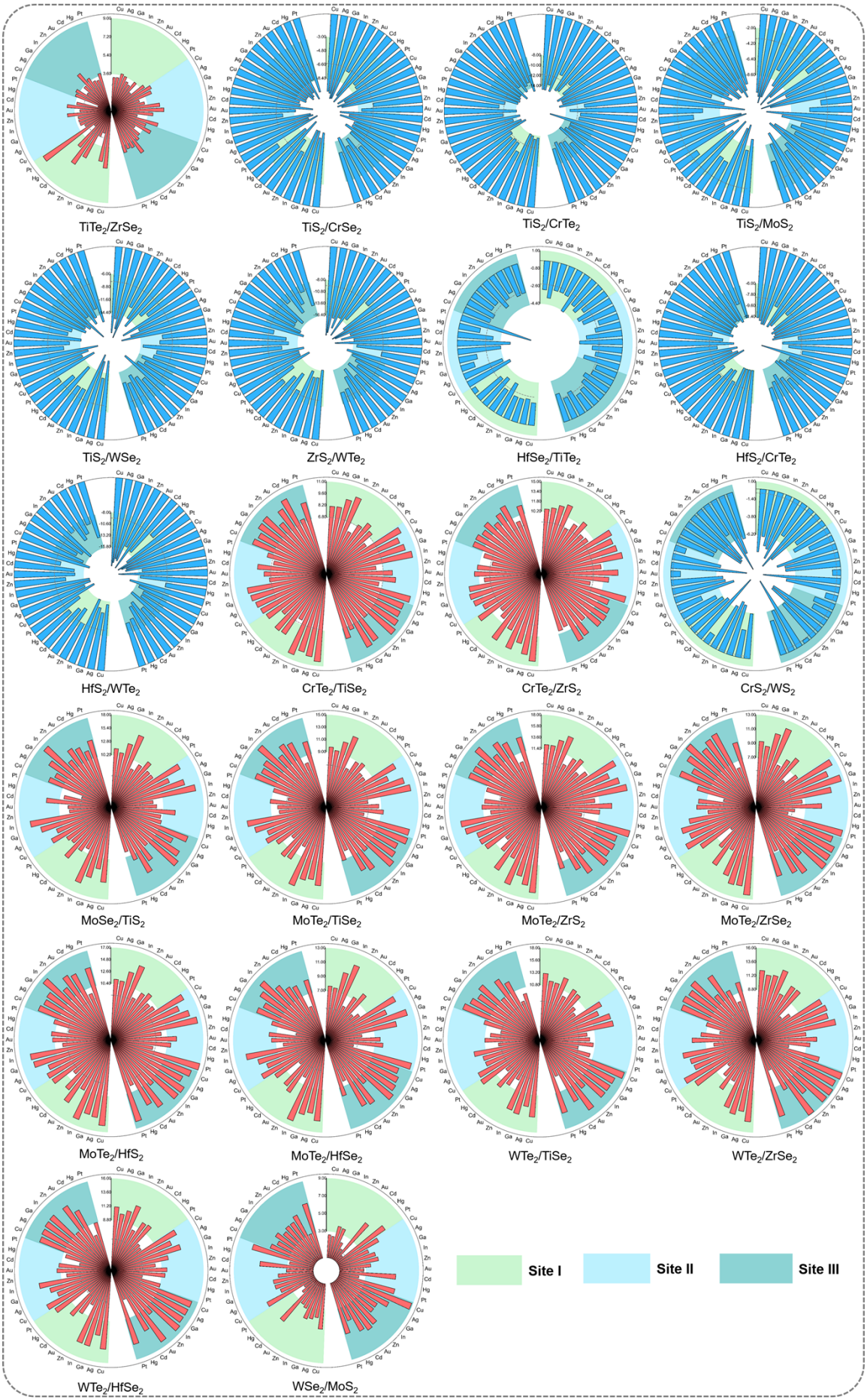
TiTe2/ZrSe2
TiS2/CrSe2
TiS2/CrTe2
TiS2/MoS2
TiS2/WSe2
ZrS2/WTe2
HfSe2/TiTe2
HfS2/CrTe2
HfS2/WTe2
CrTe2/TiSe2
CrTe2/ZrS2
CrS2/WS2
MoSe2/TiS2
MoTe2/TiSe2
MoTe2/ZrS2
MoTe2/ZrSe2
MoTe2/HfS2
MoTe2/HfSe2
WTe2/TiSe2
WTe2/ZrSe2
WTe2/HfSe2
WSe2/MoS2
Site I
Site II
Site III

Figure S8. Radial bar plots of out-of-plane polarization for the remaining 22 AC(CA) stacked heterobilayers that do not exhibit switchable out-of-plane polarization. In these structures, both stacking configurations show polarization in the same direction, indicating the absence of sliding ferroelectric behavior. The visualization follows the same convention as in the main text: red and blue bars represent positive and negative polarization values, respectively, while background colors distinguish the intercalation sites. All OOP values are reported in pC/m.

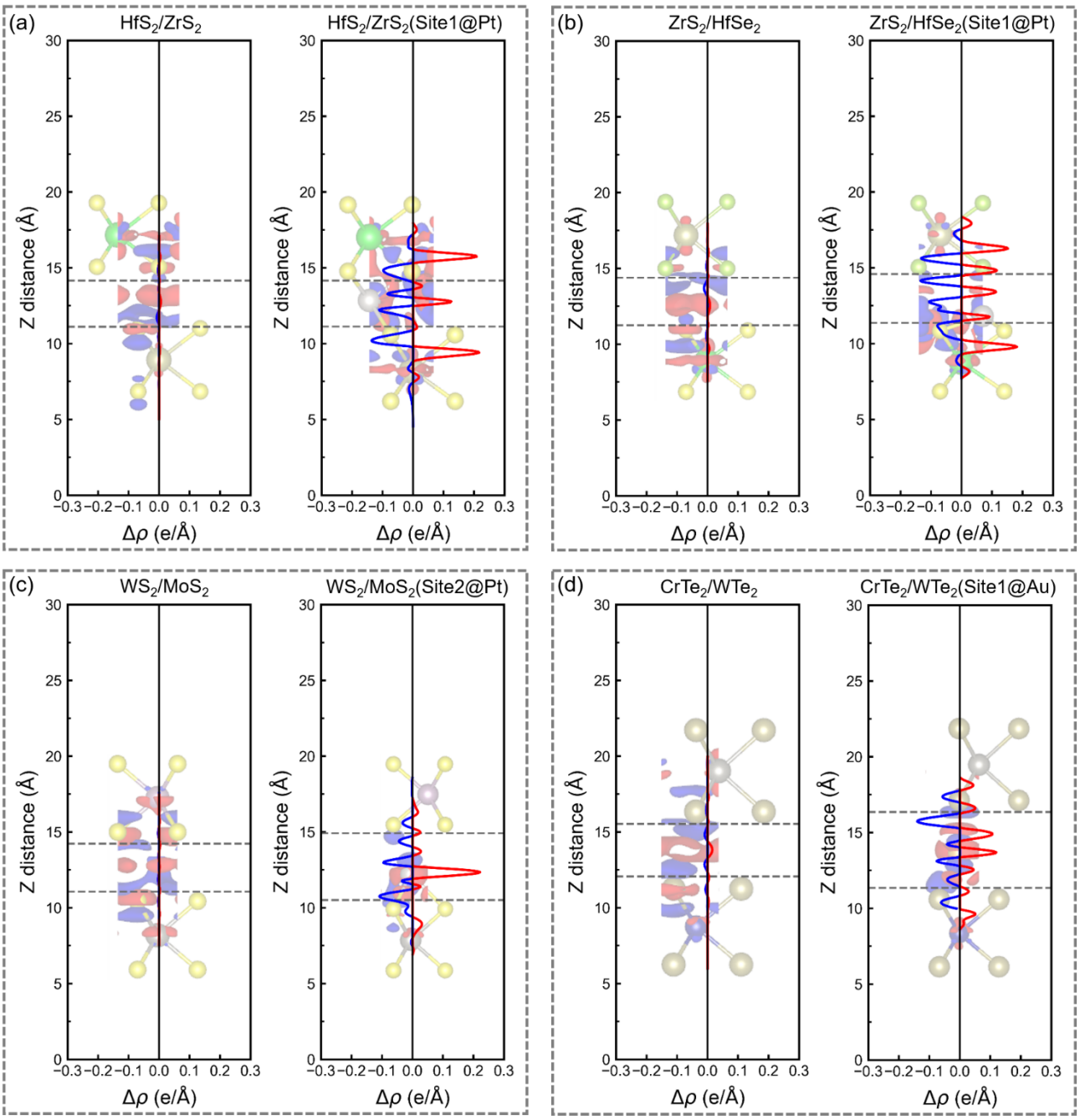

Figure S9. Charge density difference (CDD) and planar-averaged CDD (PA-CDD) for four representative systems: (a) HfS_2/ZrS_2; (b) $ZrS_2/HfSe_2$; (c) WS_2/MoS_2; (d) $CrTe_2/WTe_2$. The left panels correspond to the pristine structures and the right panels to the intercalated counterparts. Blue regions indicate electron accumulation, while red regions denote electron depletion.

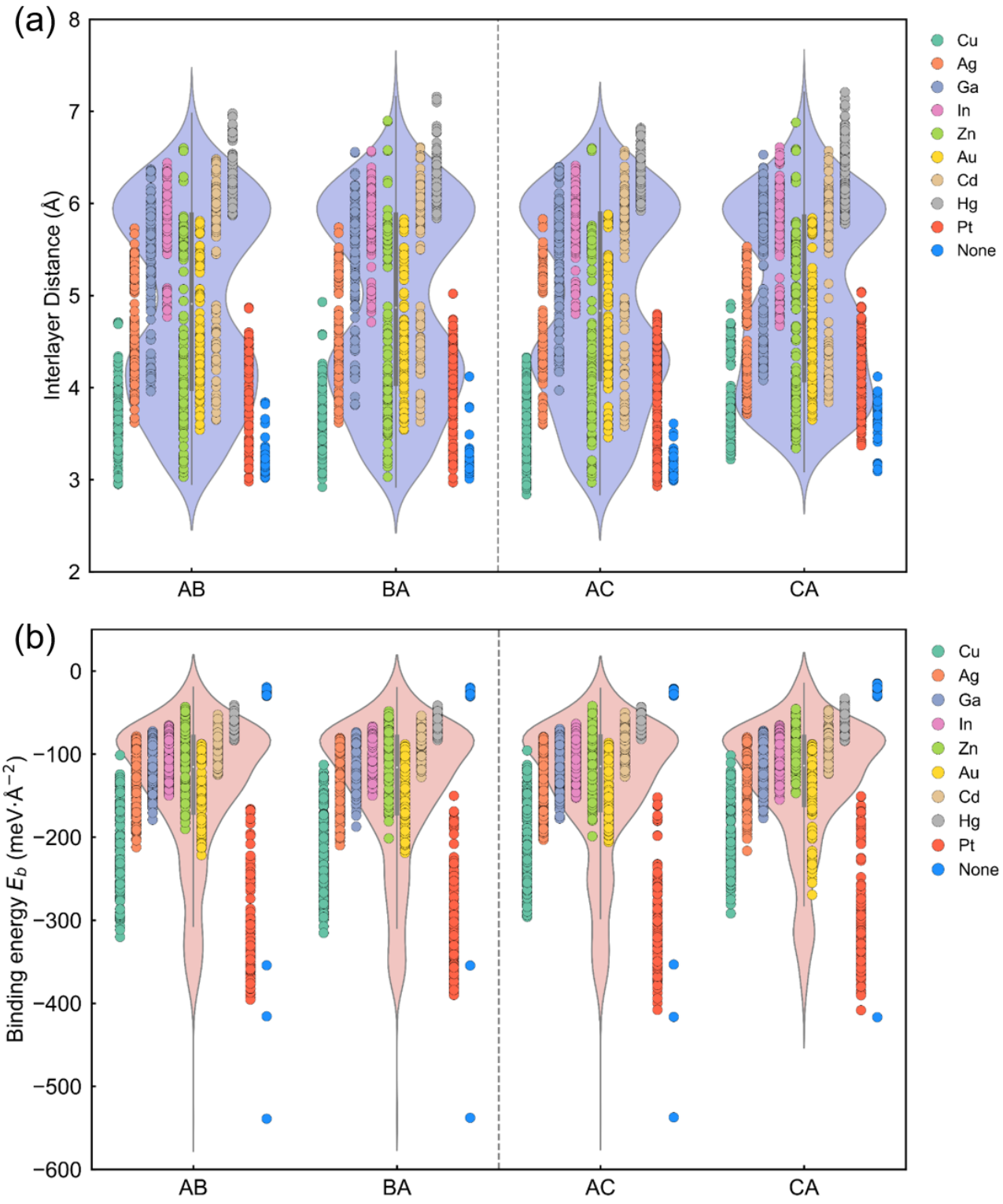

Figure S10. (a) Violin plot of interlayer distances for bilayer heterostructures with various intercalants and the non-intercalated case. (b) Violin plot of interfacial binding energies for the same systems. Each point represents a specific structure.

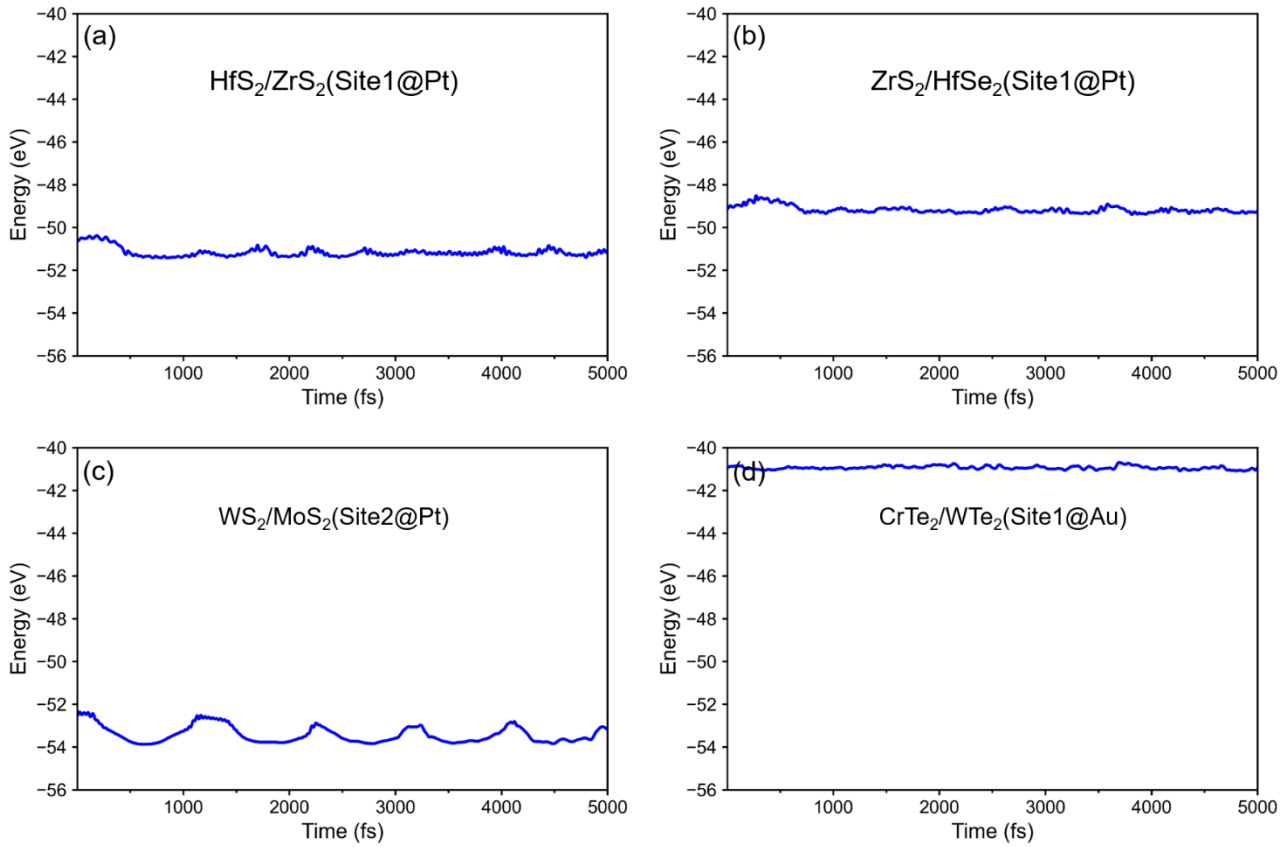

Figure S11. Time evolution of the total energy from ab initio molecular dynamics (AIMD) simulations in the NVT ensemble at 300 K for four representative intercalated TMD heterobilayers: (a) HfS_2/ZrS_2 (Site1@Pt); (b) $ZrS_2/HfSe_2$(Site1@Pt); (c) WS_2/MoS_2(Site2@Pt); (d) $CrTe_2/WTe_2$(Site1@Au).

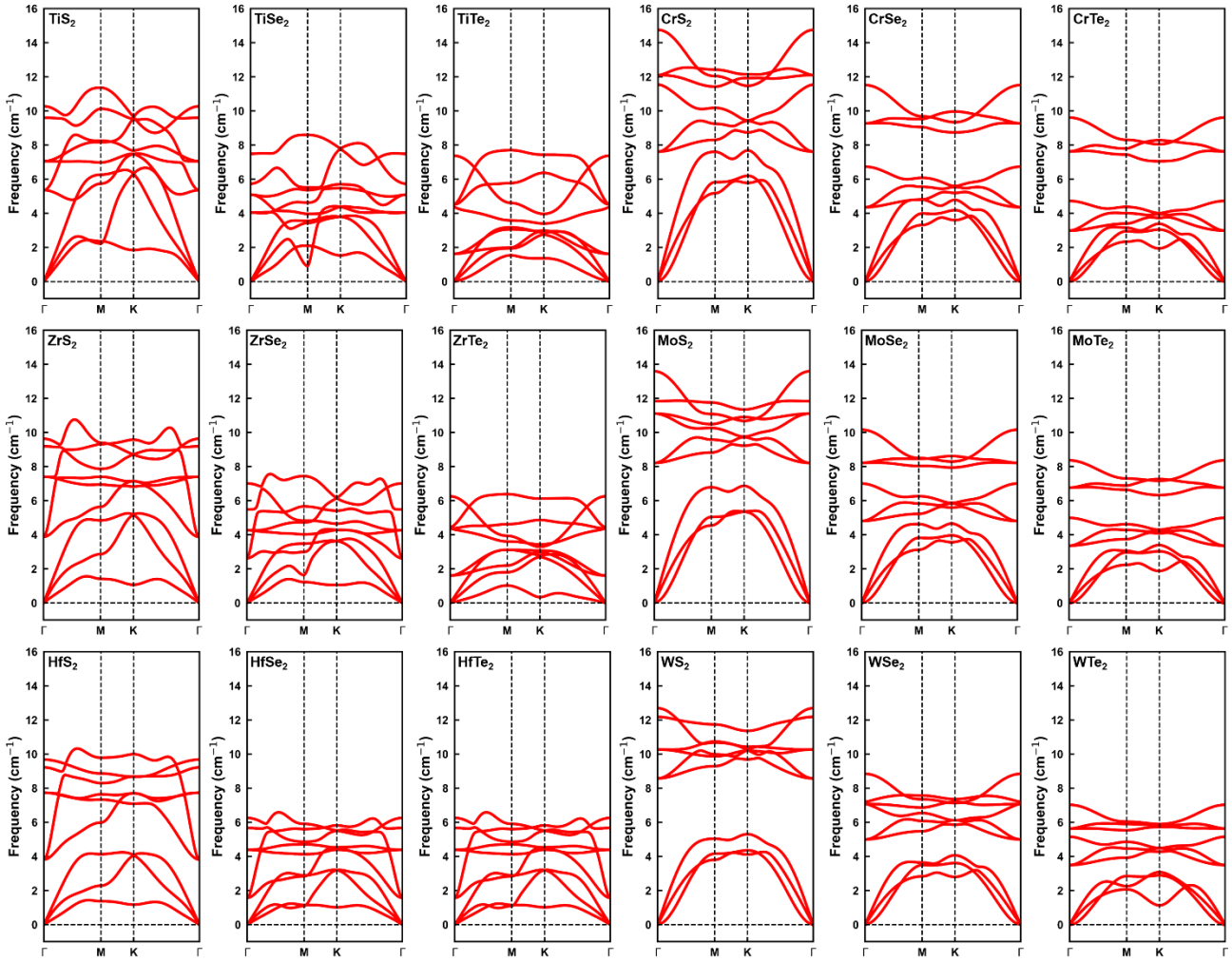

Figure S12. Phonon dispersion relations of the 18 pristine TMD monolayers used as building blocks for the heterobilayers.

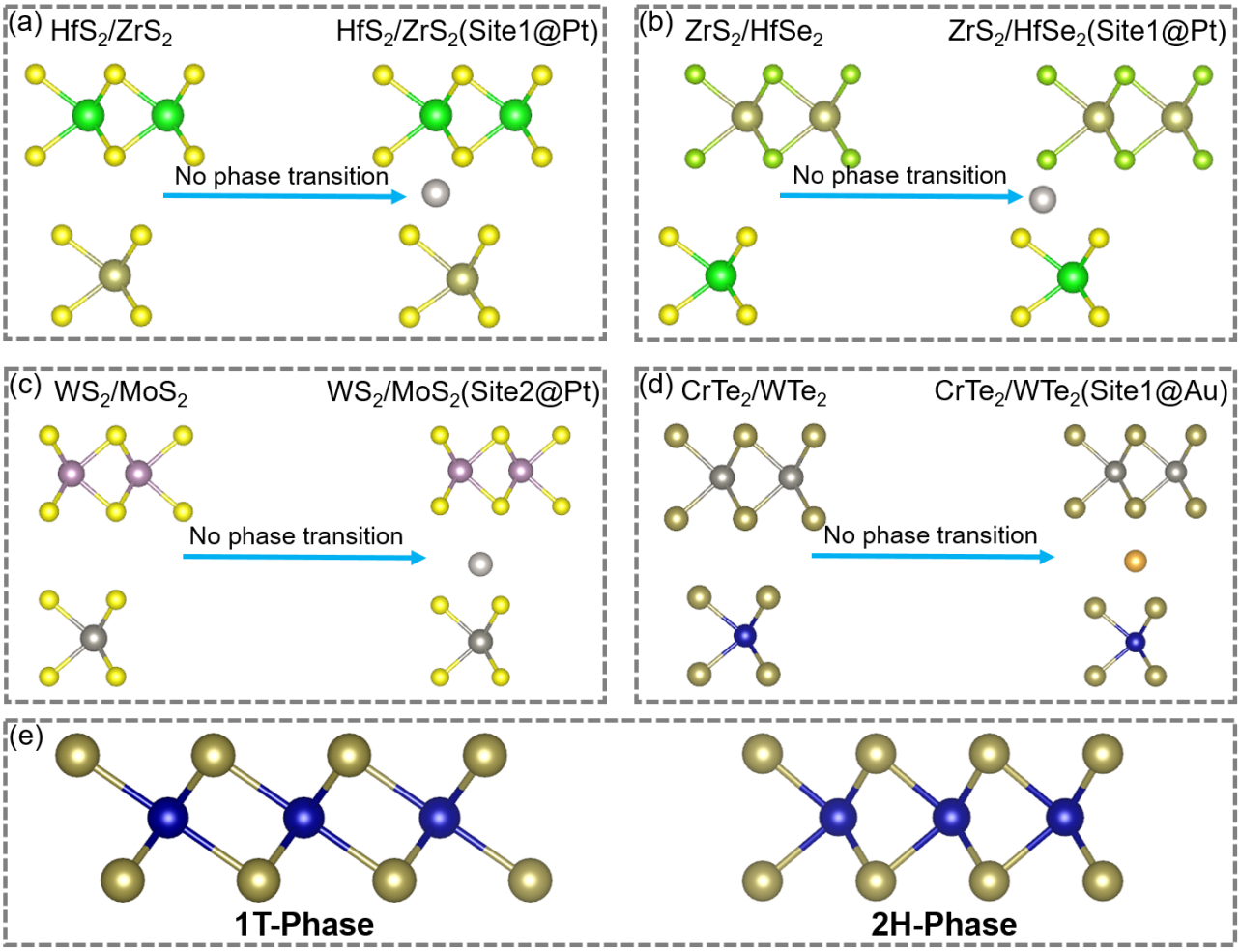

Figure S13. Schematic illustrations of four representative heterostructures before and after intercalation: (a) HfS_2/ZrS_2, (b) $ZrS_2/HfSe_2$, (c) WS_2/MoS_2, and (d) $CrTe_2/WTe_2$. The left panels show the relaxed structures before intercalation, while the right panels correspond to the relaxed structures after intercalation. Notably, all systems preserve their original crystal phases upon intercalation, with no phase transition observed. (e) Schematic representations of the typical 1T phase (left panel) and 2H phase (right panel) of transition metal dichalcogenides.

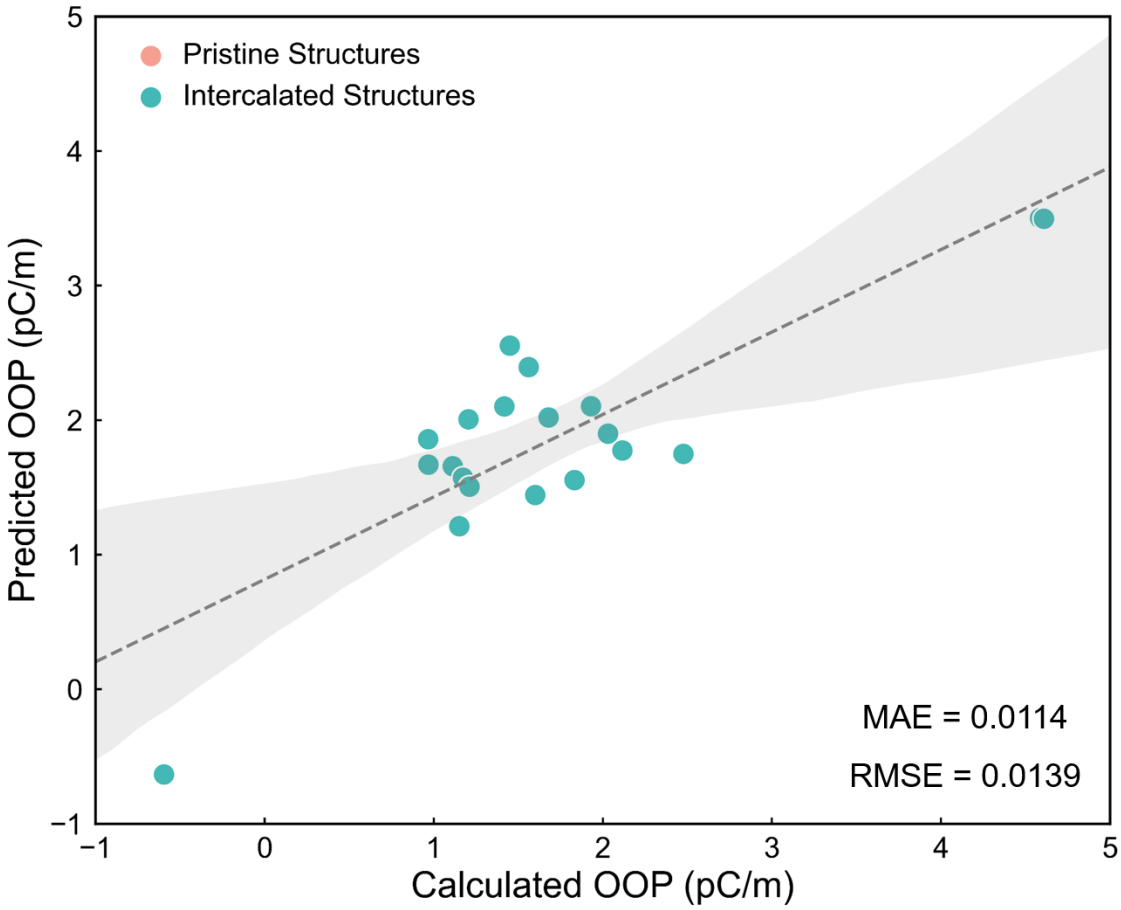

Figure S14. Parity plot comparing CEGNN-predicted and DFT-calculated out-of-plane polarization (OOP) for the additional test set of 20 intercalated TMD heterobilayers.